

University of Texas Rio Grande Valley

ScholarWorks @ UTRGV

Theses and Dissertations

12-2021

The Skeletal Structure of Hot Mix Asphalt and the Effects of Fiber Additives

Samantha A. Avila

The University of Texas Rio Grande Valley

Follow this and additional works at: <https://scholarworks.utrgv.edu/etd>



Part of the [Civil and Environmental Engineering Commons](#)

Recommended Citation

Avila, Samantha A., "The Skeletal Structure of Hot Mix Asphalt and the Effects of Fiber Additives" (2021).
Theses and Dissertations. 821.

<https://scholarworks.utrgv.edu/etd/821>

This Thesis is brought to you for free and open access by ScholarWorks @ UTRGV. It has been accepted for inclusion in Theses and Dissertations by an authorized administrator of ScholarWorks @ UTRGV. For more information, please contact justin.white@utrgv.edu, william.flores01@utrgv.edu.

THE SKELETAL STRUCTURE OF HOT MIX ASPHALT
AND THE EFFECTS OF FIBER ADDITIVES

A Thesis

by

SAMANTHA A. AVILA

Submitted in Partial Fulfilment of the
Requirements for the Degree of
MASTER OF SCIENCE

Major Subject: Civil Engineering

The University of Texas Rio Grande Valley

December 2021

THE SKELETAL STRUCTURE OF HOT MIX ASPHALT
AND THE EFFECTS OF FIBER ADDITIVES

A Thesis
by
SAMANTHA A. AVILA

COMMITTEE MEMBERS

Dr. Phillip Park
Chair of Committee

Dr. Thang Pham
Committee Member

Dr. Yooseob Song
Committee Member

December 2021

Copyright 2021 Samantha A. Avila

All Rights Reserved

ABSTRACT

Avila, Samantha A., The Skeletal Structure of Hot Mix Asphalt and the Effects of Fiber Additives. Master of Science (MS), December, 2021, 70 pp., 12 tables, 29 figures, references, 57 titles.

Hot mix asphalt (HMA) has proven to be successful in providing a proper paving surface for transportation services throughout the world. Asphalt pavement could be altered as the gradation of the mixture is adjusted. For instance, mixtures could vary from Dense Graded (DG) that contain a fairly even percentage of all aggregate size allowing for a more compact fit to Stone Matrix Asphalt (SMA) where the coarse aggregate compromise the main skeleton while fine aggregate fills the voids. This study investigates the effects of fibers and skeletal structures on mechanical properties of HMA. Two types of fiber additives are tested on both DG and SMA mixtures. The specimens were fabricated based on SuperPave design method and the same amount of compaction efforts were given to both control and fiber reinforced specimens. A set of indirect tension tests were conducted at room temperature to examine the cracking resistance of fiber reinforced HMA. The results showed that the addition of fibers improves the fracture energy, post-cracking energy, and toughness of HMA. The fiber reinforced SMA had a greater improvement than DG. On the other hand, decreases in indirect tensile strength were observed in fiber reinforced HMA. The results presented in this study show that 1) adding fibers has potential to improve cracking resistance of HMA and 2) special cares in compaction and determination of optimum binder content will be needed to achieve proper air-void contents.

DEDICATION

The completion of my thesis is dedicated to all my former educators, friends and family. Without the knowledge, support and guidance that has been given to me, this would not have been possible. A special dedication to my mother who has been my biggest support, mentor and the person I strive to be. I appreciate your unwavering love and support.

ACKNOWLEDGMENTS

This thesis was the result of the contributions of many people. To begin, I would like to give the greatest acknowledgements and express my sincere gratitude towards Dr. Philip Park for allowing me to conduct this study and guiding me with his knowledge and experience. Further gratitude is given to the members of my thesis committee Dr. Thang Pham and Dr. Yooseob Song. The input given has allowed for the best-quality research.

Recognition must also be given to those who assisted such as the employees of MEG Engineering, in specific Juan Borjon, Salma Martinez, Humberto Palma and Andres Palma. Also, appreciation is given to Franher Cantu who assisted my research for two semesters and dedicated time in the laboratory with me.

TABLE OF CONTENTS

	Page
ABSTRACT.....	iii
DEDICATION.....	iv
ACKNOWLEDGMENTS.....	v
TABLE OF CONTENTS.....	vi
LIST OF TABLES.....	ix
LIST OF FIGURES.....	x
CHAPTER I. INTRODUCTION.....	1
1.1 Background.....	1
1.2 Statement of Problem.....	3
1.3 Objective of Research.....	4
1.4 Methodology.....	5
1.5 Thesis Outline.....	5
CHAPTER II. CHARACTERISTICS OF FIBER REINFORCED ASPHALT.....	7
2.1 Introduction.....	7
2.2 Mechanical Properties.....	7

2.3 Skeletal Structure.....	12
2.4 Fibers.....	15
2.5 Asphaltic Binders.....	20
2.6 Fiber-Aggregate-Binder Interlocking.....	25
2.7 Fatigue Testing.....	27
2.8 Design.....	32
2.9 Degradation of Asphalt.....	34
2.10 Conclusion.....	36
CHAPTER III. MATERIALS AND EXPERIMENTAL METHODS.....	37
3.1 Raw Material.....	37
3.2 HMA Design.....	38
3.3 HMA Specimen Preparation.....	41
3.4 HMA Testing.....	44
CHAPTER IV. INVESTIGATION OF HOT MIX ASPHALT AND THE EFFECTS OF FIBER ADDITIVES	46
4.1 Production of Fiber Reinforced Hot Mix Asphalt.....	46
4.2 Investigation of Fiber Additives.....	57
4.3 Discussions on the effects of fiber additives on HMA.....	60
CHAPTER V. CONCLUSION AND FUTURE WORK.....	63
5.1 Conclusion.....	63

5.2 Recommendations for Future Work.....	64
REFERENCES.....	65
BIOGRAPHICAL SKETCH.....	70

LIST OF TABLES

	Page
Table 3.1: Properties of fibers.....	38
Table 3.2: Dense mixture D-5 Standard for grading of total aggregate	39
Table 3.3: Stone Matrix Asphalt SMA-D medium gradation limits.....	39
Table 3.4: Minimum and maximum boundaries of sieve size for nominal maximum aggregate size.....	40
Table 4.1: Gradation curve for (a) DG asphalt mixtures (b) SMA mixtures.....	47
Table 4.2: Bulk specific gravity of DG, DG SF 0.2-13, DG HF 0.55-33.....	49
Table 4.3: Bulk specific gravity of SMA, SMA SF 0.2-13, SMA HF 0.55-33.....	50
Table 4.4: Theoretical maximum specific gravity of DG, DG SF 0.2-13, DG HF 0.55-33.....	52
Table 4.5: Theoretical maximum specific gravity of SMA, SMA SF 0.2-13, SMA HF 0.55-33.....	53
Table 4.6: Air void percent of DG, DG SF 0.2-13, DG HF 0.55-33.....	54
Table 4.7: Air void percent of SMA, SMA SF 0.2-13, SMA HF 0.55-33.....	55
Table 4.8: Summary of ITS, FE, PE and toughness for DG and SMA	62

LIST OF FIGURES

	Page
Figure 2.1: Variation of (a) indirect tensile strength and (b) toughness of flattened and twisted steel fibers.....	8
Figure 2.2: Effect of fibers on (a) stability values and (b) flow.....	9
Figure 2.3: Comparison of fatigue life for various mixtures.....	11
Figure 2.4: Stress-Strain curves of fiber reinforced asphalt concrete.....	12
Figure 2.5: Graphical definition of three-particle size range.....	13
Figure 2.6: Relationship between stress p and aggregate size: (a) $D= d=D_o$ (b) $D=19$ mm (c) $d=0.3$ mm.....	15
Figure 2.7: Comparison of pull-out force-displacement curves of (a) matrix failure mode (b) interface failure mode (c) mixed mode failure.....	17
Figure 2.8: (a) Resilient modulus and (b) permanent strain results for different fiber content..	18
Figure 2.9: Micrographs showing visually apparent (a) poor, (b) average, and (c) good aqueous dispersions correlating with model results.....	19
Figure 2.10: Specifications and greatest improvements of different types of fibers used in HMA.....	20

Figure 2.11: Uniaxial tension stress test (UTST) tensile strength.....	22
Figure 2.12: Load vs displacement curve of bitumen under mode 1, mode 2 and mixed mode.....	23
Figure 2.13: Carbon monoxide release curves for SBS, FRC, FRC-Si asphalt.....	24
Figure 2.14: Schematic view of the reinforcing mechanism.....	26
Figure 2.15: Summary of fatigue test characteristics.....	28
Figure 2.16: Wohler's diagram of the asphalt mixture 1.....	30
Figure 2.17: Loading method and model diagram.....	31
Figure 2.18: Block Diagram of the Design Subsystems.....	34
Figure 3.1: (a) Limestone grade 4, 5 and 6 stockpiles (b) closer view of stockpile.....	37
Figure 3.2: (a) SF 0.2-13 in asphaltic mixture (b) HF 0.55-33 in asphaltic mixture.....	41
Figure 3.3: Specimen preparation (a) aggregate mixture (b) heated asphalt (c) combination of heated aggregate and asphalt (d) sample molds.....	43
Figure 3.4: (a) Gilson HM-398 Load Frame and Karol Warner Data Readout (b) zoomed view of loading plates.....	45
Figure 3.5: ITS, FE and PE description.....	45
Figure 4.1: Gradation curve for (a) DG asphalt mixtures (b) SMA mixtures.....	46
Figure 4.2: ITS vs strain curve for (a) DG (b) DG SF 0.2-13 (c) DG HF 0.55-33.....	56

Figure 4.3: ITS vs strain curve for (a)SMA (b) SMA SF 0.2-13 (c) SMA HF 0.55-33..... 57

Figure 4.4: (a) Broken fiber reinforced HMA specimens after ITS test (b) Fractured
surface of SF 0.2-13 (c) Fractured surface of HF 0.55-33..... 58

Figure 4.5: ITS vs strain curve for averaged (a) DG, DG SF 0.2-13, DG 0.55-33 (b) SMA,
SMA SF 0.2-13, SMA 0.55-33..... 59

Figure 4.6: FE, PE and toughness for averaged (a) DG, DG SF 0.2-13, DG 0.55-33
(b) SMA, SMA SF 0.2-13, SMA 0.55-33..... 60

CHAPTER I

INTRODUCTION

1.1 Background

Asphaltic mixtures were created far before they began being used to construct roadway pavement material. However, once it got its start, it rapidly became the most widely used paving material all over the world (O’Flaherty and Hughes 2015). In the United States, about 94% of roadway systems consist of asphalt (National Asphalt Pavement Association 2013) . The challenge is not associated with producing the pavement but rather with maintaining the pavement at a high-quality standard for a long period of time (Liu et al. 2020). For this reason, additives were introduced into asphaltic mixtures to provide additional reinforcement to absorb the stress being produced by traffic loads (Abtahi et al. 2010; Shukla et al. 2014 Meng et al. 2020; Xu et al. 2010)

Dating back to ancient times, the use of straw or animal wool and hair was a typical technique for the construction of a plethora of structures to provide additional stability. In southwest America and central Mexico, pueblo houses were built by incorporating straw into a clay mixture that was used as the composite to form bricks. Vargas et al. (1986) confirmed that the straw provided additional reinforcement during the binding process and also allowed for the material to dry evenly and prevent cracking of the bricks due to uneven expansion and contractions when they were used for buildings. Kennedy et al. (2013) studied the effects of

horse hair used in lime plasters. He reassured that horse hair was a common additive into plasters because of the durability, stiffness and thermal comfort properties it provides. It also acts as a bridging agent to control shrinkage and expansion of the plaster, which enhances the performance and lifetime of the asphalt.

The first known study conducted on the reinforcement on definite asphalt came from Zube (1956) who studied the effects of wire mesh on roadway pavement. He conducted a large-scaled experiment in which 8 types of wire mesh (variations of expanded metal mesh, bituminous road mesh, welded wire fabric) were used in a 4-inch bituminous resurfacing. It was concluded that wire mesh, regardless of the type, had positive consequences. Longitudinal cracks were not produced to the extent that typical asphalt pavement experiences. It was concluded that the inclusion of reinforcement in asphalt mixture did in fact cause strengthening in the pavement that could prevent crack formations and expansions.

As time has progressed, studies on reinforced asphalt grew with each one adapting to the initial results obtained regarding the reinforcement of asphalt provided by Zube (1956). The effects of many individual fiber types have been examined with differing asphaltic mixes such as stone matrix asphalt, open-graded asphalt, or dense-graded asphalt. Additional research has focused on the optimization of the asphalt mixtures and of the fibrous material. Reinforcement can be provided by a remarkable number of fibers of diverse properties: natural or synthetic; fibers, strips, sheet grids or bars; rough or smooth; stiff or elastic. The use of fibers as such in asphaltic mixtures has impacted pavement performance and sparked a flame for further studies on the effects of fiber types, shapes, and sizes. Each study providing new information for the following to continuously produce results that effect the asphalt pavement that is being used on actual roadways.

Fiber Reinforced Asphalt (FRA) is an asphalt concrete composite with additional reinforcement provided by fiber additives. The inclusion of high tensile strength fibers can improve the stability of the composite material and allow it to withstand a higher strain energy. The increase in tensile strength is produced as a result of higher cohesion throughout the mix. This can in turn enhance the ductility and strengthen the resistance to fatigue, cracking, rutting, moisture damage and bleeding. The properties of FRA can be determined by designing proper interactions between the fiber and matrix interface.

In some cases, fibers in the asphaltic mixture act as a filler such as fine aggregates in order to prevent drain down as well as defects and deformations of the composite. Although its main purpose is not to entirely impede cracking, fibers can decelerate cracking propagation during the fatigue and fracture process. FRA has a great potential to improve the quality of asphalt pavements that provide a high safety level of civil infrastructure.

1.2 Statement of Problem

Roadways are paved in order to provide a smooth riding surface with suitable friction for all types of transportation. Most importantly, asphalt pavement must be able to provide a surface that can withstand the loads and stresses being applied. Asphalt concrete is a type of pavement that has been widely used for years. However, many defects can be produced in the pavement over time. The significant growth in population and transportation of goods and people demands more reliable pavement structures.

Former studies have proved that the use of fiber additives in asphalt concrete can improve the stability of pavement. Mixtures consisting of the fibers have produced significant results

showing substantial resistance to deformation of asphalt pavement. The fiber additives provide an interlocking concept within the skeletal structure of the asphalt that can prevent or delay cracking. This can hinder the pavement from producing reflective cracks, which later produce the surface defects visible to the human eye. Improvements of asphaltic mixtures must improve concurrently with the increase of population and the loads being applied by the traveling public on the pavement. It is important that high pavement performance is produced from asphalt concrete pavements otherwise constant maintenance projects will have to be administered, which will be very costly to the owner.

The design of FRA has varied widely depending on the environmental conditions and the traffic loads that the asphalt pavement was being constructed for. Nonetheless, the results have been consistent and have shown that asphalt concrete including the fiber additives have shown substantial improvement to the longevity of the pavement structure. Therefore, this research aims investigate the qualities of different asphalt gradations and determine the effects of fiber additives on the respective mixture types.

1.3 Objective of Research

The research being conducted aims to investigate the effects of fiber additives on the mechanical properties of different asphalt pavements varying in gradation type. Since the main interest of the study is on improvements in cracking resistance of HMA, indirect tension tests will be conducted at room temperature for the various samples. The effects of fiber additives and skeletal structures on mechanical properties of HMA will be examined. The findings will provide

fundamental background information on the practical and effective ways to improve HMA performances using fibers.

1.4 Methodology

The research was initiated by collecting previous investigations that were analyzed to understand the property changes that most benefit asphalt strength. Thereafter, non-reinforced and fiber reinforced specimens were fabricated based on the SuperPave design method. Indirect tension tests will be conducted on samples with different aggregate gradations and containing two fiber types. Finally, the indirect tension test results will be studied to make a final conclusion on the effects of fiber additives to dense-graded asphalt and stone matrix asphalt.

1.5 Thesis Outline

The following thesis consists of 5 chapters. Chapter 1 gives an introduction to the topic of FRA by giving background, current problems, objective and methodology of this research. Chapter 2 gives further insight through a literature review on various topics: mechanical properties, skeletal structure, fibers, asphaltic binders, fiber-aggregate-binder interlocking, fatigue testing, design and degradation of asphalt. In Chapter 3, it explains the materials and methodology that will be used throughout the research. Chapter 4 explains the process of producing HMA samples and tests to determine sample properties such as bulk specific gravity, maximum theoretical specific gravity, and air void percentage. It also discusses the effects of the fiber additives by showing the data on fracture energy, post-cracking energy, and toughness

obtained from indirect tension tests. Chapter 5 gives a brief summary of conclusions and gives recommendations for future work.

CHAPTER II

CHARACTERISTICS OF FIBER REINFORCED ASPHALT

2.1 Introduction

As previously mentioned, FRA has become a highly used composite material used in the construction of roadway pavements in order to maintain high performance levels over a large time frame (Abtahi et al. 2010; Wu et al. 2008; Button and Lytton 1987). By modifying the skeletal structure, fiber types, fiber-binder-aggregate interlocking characteristics and mixing process, an increase in the strength parameters can be produced (Button and Lytton 1987, Xu et al. 2010). Reinforcement in an asphalt matrix can change the viscoelasticity of mixture; improve dynamic modulus, moisture susceptibility, creep compliance, rutting resistance and freeze-thaw resistance; while they reduce the reflective cracking (Abtahi et al. 2010; Shukla et al. 2014 Meng et al. 2020; Xu et al. 2010). Precise optimization will also lead to the production of asphaltic mixtures suitable to use in construction and consequently lead to safe and reliable pavement for the transportation of people and goods around the world.

2.2 Mechanical Properties

Asphalt pavements undergo large, reoccurring loads produced by the traveling public. In order to maintain good conditions despite the constant stresses it is experiencing, the asphalt mixture must be composed of strong mechanical properties. FRA has become common in

construction due to the improvement of strength parameters that it provides. These properties allow the pavement to remain durable after repeated loading for long periods of time. This allows for safer and reliable roadways, which is the ultimate goal.

Park et al. (2015) examined the cracking resistance of fibers in asphalt concrete through indirect tensile tests. The stress-strain graphs provided 4 different values that were utilized to analyze the overall results: fracture energy, post-cracking energy, toughness, indirect tensile strength. The fracture energy and indirect tensile strength are the best index of the cracking resistance before prominent cracking occurs. On the other hand, the post-cracking energy is an indicator of how cracking will spread or continue after major cracking takes place. These properties were evaluated for each FRA sample that was tested to determine the best type of fibers to use. The indirect tensile strength and toughness graphs of FRA samples containing flattened and twisted steel fibers are shown in Figure 2.1. The outcomes of the tests proved that the mechanical properties of the asphalt can be significantly improved for FRA materials. Even further enhancements can be produced to resist cracking if proper optimization is completed for each material, especially that of fibers.

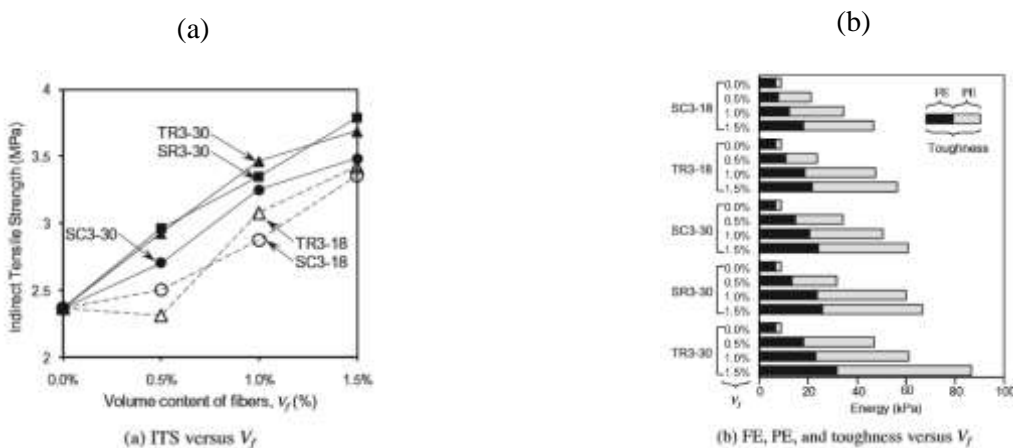


Figure 2.1. Variation of (a) indirect tensile strength and (b) toughness of flattened and twisted steel fibers (Park et al. 2015)

The use of roofing waste polyester fibers for FRA mixtures was studied by Anurag et al. (2009) to determine the effects on mechanical properties. Testing was conducted on several mixtures to obtain the indirect tensile strength, toughness and moisture susceptibility of the FRA material. Optimization of the fiber length and percentages was also conducted on this study. However, the results of the fiber additives were consistent regardless of fiber type. They proved that the use of roofing waste polyester fibers causes an increase in indirect tensile strength and toughness of the composite material and decrease the moisture susceptibility. Consequently, improving the quality and longevity of asphalt pavement produced using the following mixture.

Polypropylene fibers are commonly used in concrete mixes; however, Tapkin (2008) thoroughly investigated the effects that the fibers have on asphaltic mixtures. A repeated load indirect tensile test was directed to obtain mechanical property parameters such as the tensile stress, elasticity modulus and strain. The additional reinforcement provided by the polypropylene fibers caused rutting resistance and a significant improvement in the quality of pavement. The reinforcement caused an increase in stability and decreased the flow values as shown in Figure 2.2. This proved that the FRA material can produce high performance asphalt concrete.

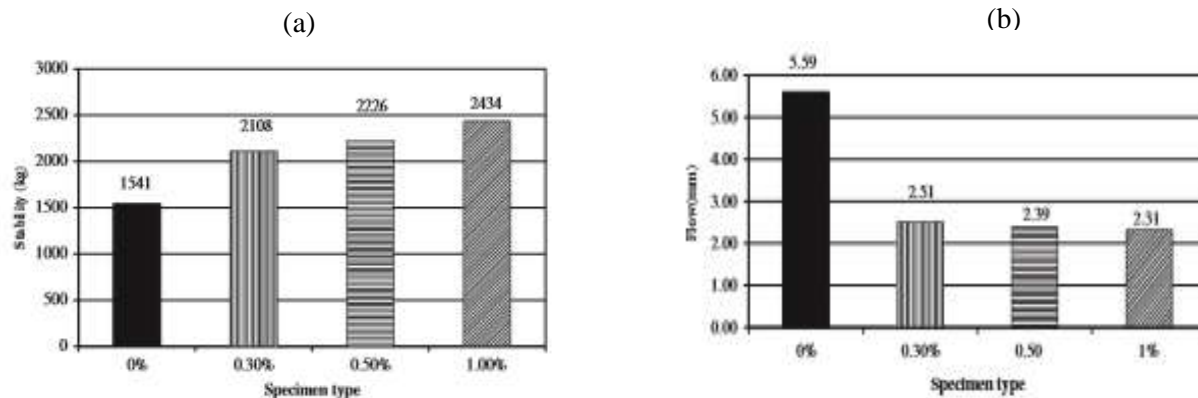


Figure 2.2. Effect of fibers on (a) stability values and (b) flow (Tapkin 2008)

Chen et al (2009) assessed the mechanical property changes of asphaltic mixtures after polyester, polyacrylonitrile, lignin and asbestos were each added into their own individual mixtures. The optimum bitumen and fiber percentages were each found for the FRA material. The durability of the composite containing the optimal properties, produced the largest increase in dynamic stability. Therefore, although all fiber additives were beneficial, the optimized fiber and bitumen properties caused a significant growth proving the fibers can generate asphalt with high levels of rutting resistance.

Jaskula et al. (2017) conducted testing on FRAC with the specific use of aramid-polyalphaolefin fibers at low temperatures. Tests were administered such as the beam bending test and semi-circle bending. The results showed that the fiber reinforcement improved the mechanical properties of the asphalt mixture at -20°C. The flexural strength and critical strain were significantly increased and the flexural stiffness was reduced. The fiber additives lead to improvements of cracking-resistance of the asphalt and proved to be a beneficial method of improving FRA pavements.

Kim et al. (1999) evaluated the reflection cracking resistance of 21 variations of FRA using polymer additives. The crack propagation was examined by applying a driving force onto asphalt composites to observe the initial cracking as well as the growth and additions of the cracks. The amount of load cycles can then be related to the fatigue life of the material. In the following study, a significant improvement to the fatigue life was seen with all the variations of the FRA as shown in Figure 2.3.

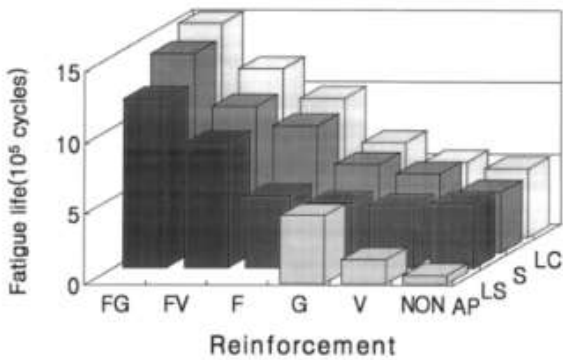


Figure 2.3. Comparison of fatigue life for various mixtures (Kim et al. 1999)

Serin et al. (2012) studied the use of steel fibers to reduce the effects of asphalt pavement under surface layer stresses. Optimization of the binder content and fiber percentage was directed to examine the largest effect on the mechanical properties. The compression levels of samples consisting of fibers decreased considerably and the optimal sample presented high stability levels. The results showed that the addition of steel fibers caused an increase in stability proving that the fibers will mediate the defects of asphalt pavement and extend the longevity.

After conducting optimization studies, Xu et al. (2010) conducted testing to determine how FRA strength properties differ to those of a plain mixture. The FRA used in this study performed at high levels in regards to strength, strain and fatigue. The stress vs strain curves in specific demonstrated an increase in indirect tensile strength for the samples with the fibers as shown in Figure 2.4. It was stated that the rutting improvement can be credited to fibers holding the asphalt at its surface even as temperatures rise, which resist the asphalt flow. Also, it reinforces the asphaltic skeletal structure by resisting shear forces within the matrix. The fatigue life and split tensile strength were additional results that showed a positive outcome due to the reinforcement of fiber additives even at lower temperatures.

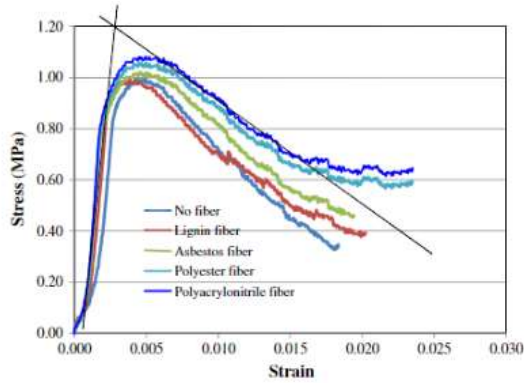


Figure 2.4. Stress-Strain curves of fiber reinforced asphalt concrete (Xu et al. 2010)

2.3 Skeletal Structure

One of the most important aspects of roadway asphalt pavement is the aggregate gradation of the mixture. The aggregates present develop stone-to-stone contact creating a skeletal structure, which support the stress acting on the matrix. The compression loads being applied onto the pavement are distributed onto the underlying soils but are all transferred differently depending on the stone-to-stone contact of the aggregates. The skeletal structure plays a huge role under high temperatures when the binder becomes less viscous. Reliant on the gradation, size, shape and angularity of the aggregate particles, different performance levels can be met and different stability properties can be developed.

The stiffness and responses of skeletal structures was examined by Zhang et al. (2019). Two identical samples were made using the same asphaltic mixture; however, the compaction efforts were different and were tested at varying frequencies. The lack of compaction in the initial mix prevents the development of stone-on-stone contact which then reduces the stiffness of the matrix. The temperature at which the mixtures are tested also affects the results due to the

property changes in the binder leaving all stability characteristics dependent of the skeletal structure.

Borrowing the theory of linear packing model established by Westman (1936), Pouranian and Haddock (2018) created a model that examines the behavior of packing systems such as a filling mechanism and occupation mechanism that can determine the rutting performance of asphalt based on the skeletal structure. In the process, they established three classifications for the range groups (Main Particle Size Range; Large Un-mixing Range; Small Un-mixing Range) as shown in Figure 2.5 for a well-graded mix based on particle diameter. It was concluded that the combination of Main Particle Size Range and Small Un-mixing Range provide the stone-on-stone contact within the mixture to maintain high levels of stability and cause resistance to rutting deformations.

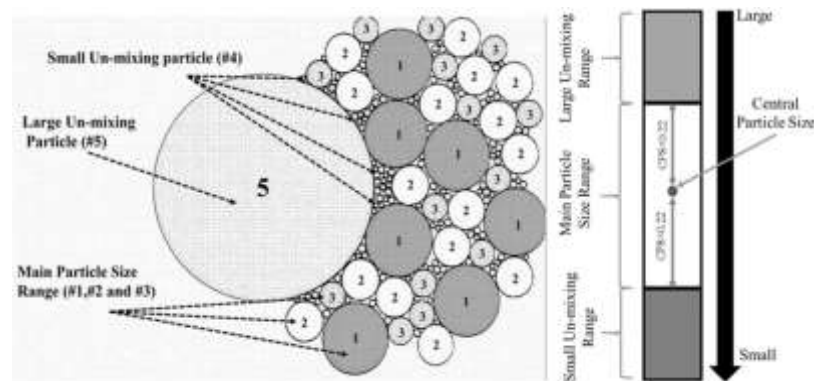


Figure 2.5. Graphical definition of three-particle size range (Pouranian and Haddock 2018)

Li (2013) developed a parameter, aggregate contact index (ACI), to analyze the contact properties of the coarse aggregate in asphalt mixtures. Li et al. (2020) used the same parameter, which uses the total number of contact points and total number of large size aggregates to establish a relationship between the ACI and stability. The results showed that a high ACI is

essential at higher temperatures where the stability relies on the aggregate interlocking, friction effect and cohesion. The skeletal structure is at its strongest when these parameters are met.

Pasetto and Baldo (2014) studied the permanent deformations of asphalt based on the design methods of the skeletal structure. The conventional optimization approach and the baileys design method were analyzed to define which produces higher performance and less resistance to deformation. Baileys method, due to the aggregate combination and interlocking, lead to higher resistance of deformations. The physical characteristics of the skeletal structure manufactured asphalt of higher quality, which would be safer if placed as asphaltic pavement.

A stress-transfer model was created by Ma et al. (2011) to examine the degradation behavior of the skeletal structure of aggregates in an asphaltic mixture. A three-dimensional stone-on-stone contacting model where aggregates of diameter d surround a single aggregate of diameter D was demonstrated. The relationship between aggregates were shown in Figure 2.6 where: (a) d and D were equal (b) where D remained constant at 19 mm and d altered in size (c) where d remained constant at .3 mm and D altered in size. The results depicted a turning point at 4.75 mm meaning that coarse aggregate provide strength to the skeletal structure and have higher stress concentrations. However, fine aggregates allow for a vast amount of contacting points and have a higher capacity of transferring stress effectively.

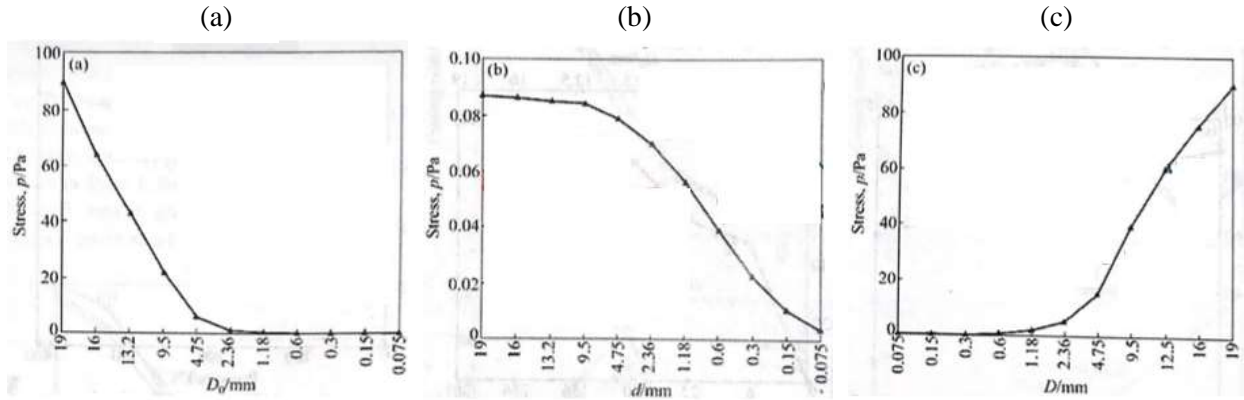


Figure 2.6. Relationship between stress p and aggregate size: (a) $D = d = D_0$; (b) $D = 19$ mm; (c) $d = 0.3$ mm (Ma et al. 2011)

Cai et al. (2018) studied the development of the skeletal structure through digital image processing by adopting the multilevel mixing method. At three stages of the mixing process, skeleton stability is examined by analyzing the contact points and inclination of the coarse aggregates. It was concluded that as the mixing stages increased, which means that smaller aggregates were incorporated into the initial maximum aggregate size. As this was conducted, the dynamic stability increased as well. Therefore, the increase in contact points, to a certain extent, caused a growth in dynamic stability.

2.4 Fibers

The use of fiber in bituminous binders and asphalt mixtures can affect the overall characteristics of the composite matrix due to their energy absorption capabilities. Asphalt concrete is prone to cracking at colder temperatures, which is when fibers have the most effect on the material. The incorporation of fibers provides a desired property in which the other material lacks. Modifying the type of fibers used in the mixture can cause further improvements

to the strength and stability of the matrix. However, optimization of the fiber type, size and shape are crucial. If the characteristics of the fiber are not chosen properly, it can have low impact and, in some cases, even cause negative results. Thorough understanding of fiber microstructure and attributes, allow for the proper adaption to reach the performance potentials of the asphalt mixture that are being sought out.

Button and Lytton (1987) conducted an analysis on the effects of engineering fabrics, synthetic fabrics and polymeric and fiberglass grids on asphalt reflection cracking. An emphasis was placed on the importance of effects that fibers will have depending on the bitumen quantity. Due to the addition of the fiber particles, the amount of asphalt included in the mixture must be increased to provide adequate coverage to the fibers as well. Each fiber type has different absorption rates and surface areas which must be accounted for during the design process to produce satisfying outcomes. If done so as it was in their testing process, the inclusion of fabrics, fibers and grids can slow down the process of cracking within the asphalt, but proper selection of the fiber types is crucial.

Park et al. (2017) examined the behavior of a single steel fiber when pulled out from the asphalt matrix. It was determined that individual fibers can each fail as one of the three pull-out modes. The three manners and the displacement vs pull out force graphs for each can be found on Figure 2.7. When the asphalt, which the fiber is embedded in, is pulled out with the fiber, it falls under the matrix failure (MaF) mode. This situation was most seen at slower pull-out speeds and at test temperatures of +20°C. The interface failure (INF) mode occurs when the fiber suddenly separates itself entirely from the asphalt binder. This was more likely to occur in faster pull-out speeds and at a test temperature of -20°C. The last mode, mixed mode failure (MMF), is a combination of the previous two modes where the fiber is partially separated from the matrix in

one section but still contains asphalt remnants in another. Results demonstrated that thinner/ shorter fibers are of greater use under high temperatures to resist rutting of the pavement. On the other hand, the longer fibers will be more beneficial under colder temperatures when ductility of the fibers is necessary.

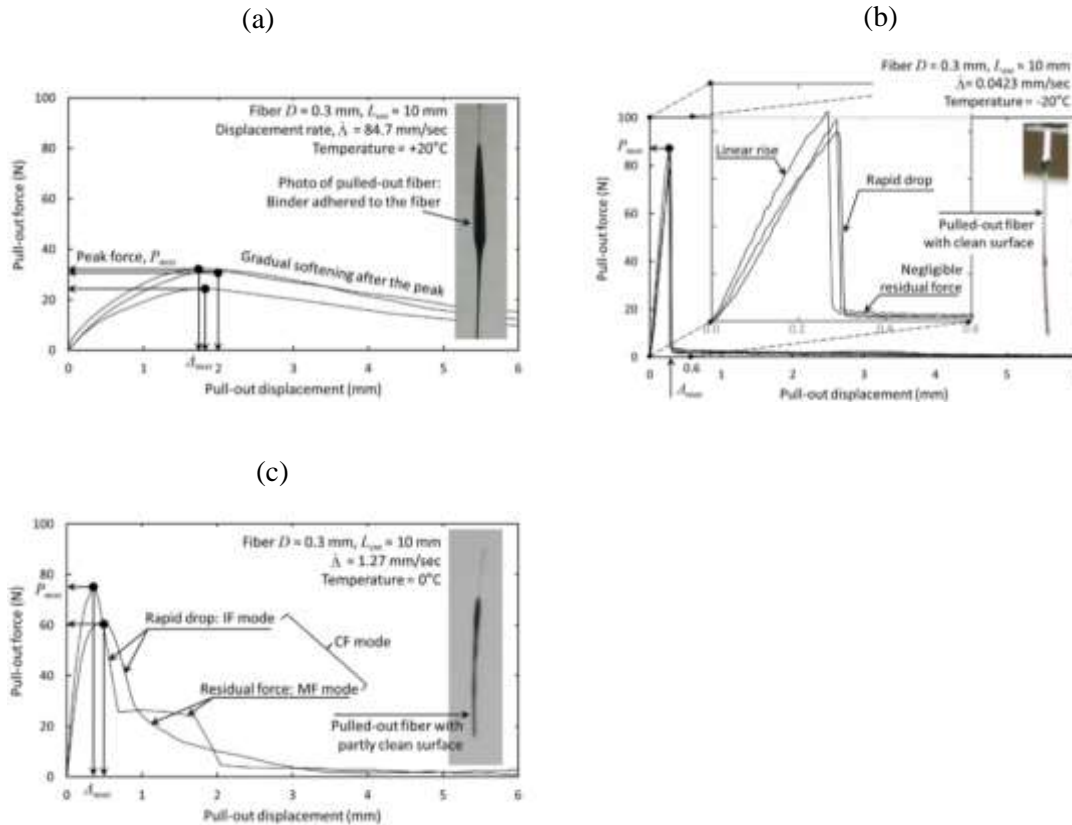


Figure 2.7. Comparison of pull-out force-displacement curves of (a) matrix failure mode (b) interface failure mode (c) mixed mode failure (Park et al. 2017)

The use of glass fibers was studied by Mahrez et al. (2005) by determining how the additives improved the results of the Marshall test, indirect tensile test, creep test and the resistance to fatigue and cracking. The results obtained as shown in Figure 2.8a demonstrate a direct relationship in which the increase in fiber percentage led to an increase of resilient modulus to a certain extent. The decrease after a certain point in the resilient modulus can be

attributed to the high percentage of fibers causing problems during the mixture process such as clumping or tangling. The creep test produced similar results (Figure 2.8b) proving that the permanent strain decreased until it hit the same turning point due to the large percentage of fibers. These results are consistent with the majority of studies conducted by other researchers who have tested other materials as well.

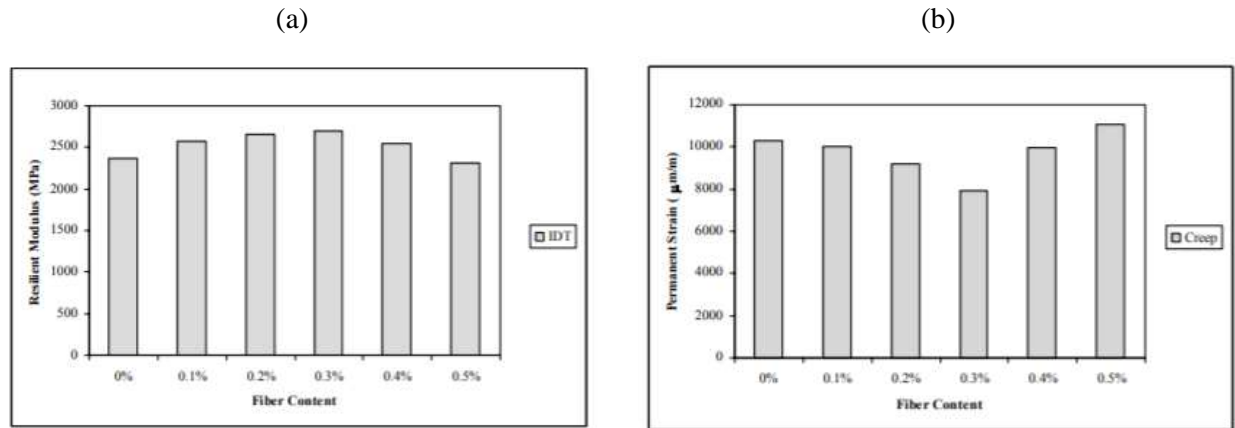


Figure 2.8. (a) Resilient modulus and (b) permanent strain results for different fiber content (Mahrez et al. 2005)

Park et al. (2015) conducted testing to optimize the fiber properties based on the reinforcing effect that steel fibers produced on asphalt concrete at a low temperature. The testing comprised of 13 combinations of various fiber types, dimensions and shape, which were each tested at 3 different content percentages. Although an increase in bitumen is necessary to properly adapt to the addition of fibers, the testing was focused solely on the effects of fibers and the bitumen increase was not accounted for. The results showed that the steel fibers with altered ends improved the post cracking strength but had no effects before the cracking process. Short and thin fibers increased the post cracking energy, yet showed no improvements to the indirect tensile strength. Longer fibers, however, produced better toughness and indirect tensile strength. It was also concluded that the fiber content must be managed correctly in order to prevent

tangling. The final conclusion established that the addition of fibers does in fact resist cracking in asphalt concrete at low temperatures.

Ensuring that fibers are distributed uniformly within the asphalt matrix plays a key role in the outcomes. Grasely and Yazdanbakhsh (2011) investigated a method of quantifying the quality of dispersion which is determined by the work inputted to reach the uniformity level. Three levels of dispersion were obtained of the carbon nanofibers in the composite material using the techniques used in the study as seen in Figure 2.9. The method used was tested and can accurately depict the results. This study can improve the fiber reinforcing in asphalt mixes by ensuring that uniform distribution is reached meaning the fibers are at the best state to contribute to the strength and stability.

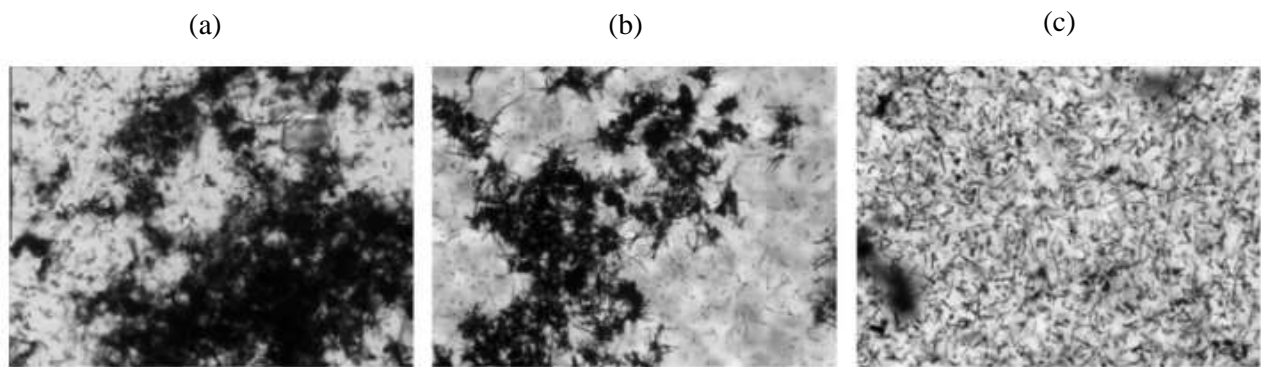


Figure 2.9. Micrographs showing visually apparent (a) poor, (b) average, and (c) good aqueous dispersions correlating with model results (Grasley and Yazdanbakhsh 2011)

Slebi-Acevedo et al. (2019) constructed a summarization of mechanical performances of fiber additives based on research conducted by different individuals. It is claimed that the most important characteristics of fibers that must be considered are tensile strength, modulus of elasticity, specific gravity and Mohs hardness. Figure 2.10 shows an overview of the most promising fibers and the maximum improvements achieved in the mechanical performance of

tests conducted in previous studies by different researchers. It was concluded that the fibers that were in all of the studies which were incorporated into this review (when added to a strong skeletal structure and proper bitumen quantities), caused positive results in the mechanical properties of asphaltic mixtures.

Fiber characteristics									Maximum improvement										
Citation	Fibers	Length (mm)	Diameter (mm)	Density (g/cm ³)	Fiber content by weight of mixture	Tensile Strength (Mpa)	Elastic modulus (Mpa)	Softening point (°C)	Rutting	MS ^b	MP ^c	Toughness	Moisture susceptibility	Fatigue life	ITS ^d	FE ^e	Dynamic stability	Complex modulus E'	Resilient modulus
[109]	Macro glass	36	0.54	2.68	0.40%	1700	72,000	860	47%	1%	23%	24%							
	Micro glass	25	0.21	2.68	0.40%			860	25%										
[82]	Aramid	19		1.45	0.05%	3000	83,000	> 450				32%	20%	20%	21%			30%	15%
[142]	Polyester	6	0.02		0.30%	531			19.57%			43.52%		57.66%		46.15%			
	Polyacrylonitrile	4.00–6.00	N/A ^a		0.30%	> 910			32.56%			61.11%		66.78%		26.92%			
	Lignin	1.1	0.045		0.30%	N/A ^a			8.43%			12.03%		40.88%		0%			
	Asbestos	5.5	N/A ^a		0.30%	30–40			11.40%			28.71%		22.52%		34.61%			
[143]	Hooked steel	30	0.4		5%	1345	210,000								63%	286%			
	Twisted steel	30	0.3		5%	1345	210,000					727%			56%	370%			
[71]	Coconut			1.18	0.30%	118	2800												8.79%
[101]	Polypropylene	6	0.04	0.91	1.0%	500	3500	160	27.50%	11.50% – 0%	11.43%				2.35%				
	Polyester	6	0.041	1.4	1.0%	1147	11,600	256		15.30%	14.28%						62.70%		
	Nylon	12	0.023	1.14	1.0%	800	3500–7000	220		8.10%	2.53%	158%					51.00%		
	Carbon	12	0.007	1.37	1.0%	4900	230,000	over 1000		0.88%		12.10%							
[95]	Polyester	6		1.4	0.35%										15%				
	Polyester	13		1.4	0.50%							117%							
[26]	Waste nylon wire	20	0.2	1.11	1%	357		220		23%			9.02%		14.89%				
[123]	Basalt		0.01–0.019	2.67	0.30%		84,000	1350	33.30%										
[45]	Carbon	5	0.01		2%	1680	752,000		2.56%	5.47%	14.65%								2.86%
[97]	Polyacrylonitrile	6	0.0013	1.18	2%		> 910	240	45.96%										
[144]	Waste polyester	13			0.50%	680		265			80%			31%					
[12]	Waste cellulose	0.5–2.00		0.52–0.56	0.50%										22%				
[77]	Nylon		12		1.00%							85%							
[145]	Polyolefin + aramid	19		0.91	0.05%	483		130		17%					11%				31%
		19		1.45		2750		450											
[134]	Aramid	19	0.012		0.07%	2700		426	139%										
[117]	Polypropylene + Aramid	19		0.91	–	483		157							25–50%	50–75%		20–50% ^f	

^aNot available.
^bMarshall Stability.
^cMarshall flow.
^dIndirect Tensile Strength.
^eFracture Energy.
^fDosage made by volume.
^gDepending on the temperature of the test.

^aNot available.
^bMarshall Stability.
^cMarshall flow.
^dIndirect Tensile Strength.
^eFracture Energy.
^fDosage made by volume.
^gDepending on the temperature of the test.

Figure 2.10. Specifications and greatest improvements of different types of fibers used in HMA (Slebi-Acevedo 2019)

2.5 Asphaltic Binders

Asphaltic binders are the most important aspect of HMA^a as it acts as the glue that binds everything together. The ratio of asphalt to aggregate as well as the type of asphalt used in the mixture play a crucial role in how it reacts to the forces that are being applied onto it. Therefore, different types of asphalt binders are being researched in order to determine which lead to the

best strength parameters. It is also important to consider how each affect the environment and what each could do to cause substantial improvements.

Pszczola and Szydlowski (2018) investigated the results on low- temperature strength properties of various bitumen types under four test methods. The first method was the Uniaxial Tension Stress Test (UTST) which gives the resultant of the maximum stress and corresponding tensile failure. The second, the Thermal Stress Restrained Specimen Test (TSRST), is a process in which the temperature is reduced at a constant rate and produces the failure stress at the failure temperature. The next was the Bending Beam Test (BBT) in which a three-point bending was easured at a constant deflection rate of 1.25 mm/min. The last test was the Semi-Circular Bending Test (SCB) in order to evaluate the fracture toughness. A total of four bitumen types were also studied with three being neat road bitumen's 35/50, 50/70, 70/100 and one Styrene-Butadiene-Styrene (SBS) modified bitumen 45/80-55. The UTST was measured at four different temperatures (except the AC11S 45/80-55). It was concluded that the decrease in temperature cause the tensile strength to increase. The mixtures with harder bitumen, 35/5 and 50/70, showed higher values of tensile strength. However, the polymer-modified binder distinctly produced a higher tensile strength overall, but was also able to produce that max strength at a much lower temperature as seen on Figure 2.11. Furthermore, the type of bitumen played a huge role on the low temperature properties of the asphaltic mixture. The SBS-modified bitumen once again proved to have the lowest value of failure temperature and highest value of failure while the 35/50 had the worst results. For the BBT, the SBS- polymer modified bitumen produced the best results but at higher temperatures did not have much impact. Lastly, the SCB once again showed similar results as the SBS-modified bitumen produced the highest fracture strength. Therefore,

the results proved that at low temperatures, the bitumen type plays a crucial role. The SBS-modified bitumen as already seen, produced the highest results across the board.

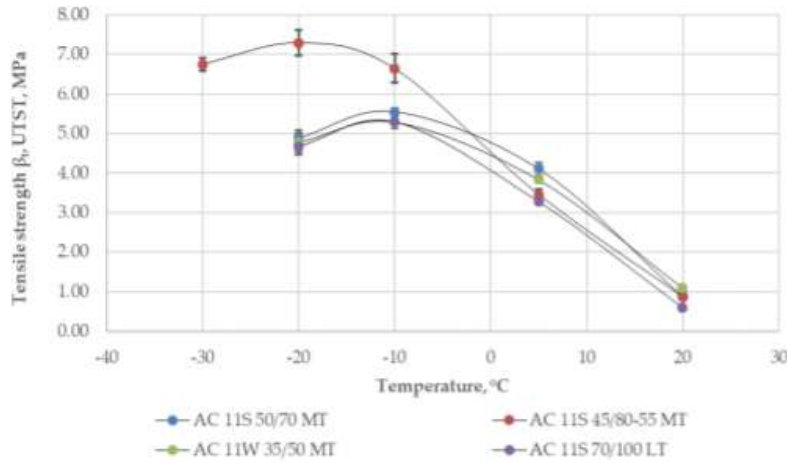


Figure 2.11. Uniaxial tension stress test (UTST) tensile strength (Pszczola and Szydlowski 2018)

Aliha (2020) examined the fracture behavior of three different bitumen types: semi-hard binder with penetration grade 30/40, soft binder with penetration grade 60/70 and polymerized bitumen modified with Styrene Butadiene Styrene (SBS). The following bitumen types were tested alone as INBB Specimens in either mode I, mode II or mixed mode I/II. The load vs displacement curves are shown in Figure 2.12. It is concluded that the fractures under mode I produced the weakest results. The overall highest load was reached with the 60/70 bitumen under mode II fracture. It was determined that as bitumen ages through RTFO, the fracture toughness of 30/40 and 60/70 decreased while the SBS bitumen was left unaffected. The bitumen type affects the fracture surface and toughness.

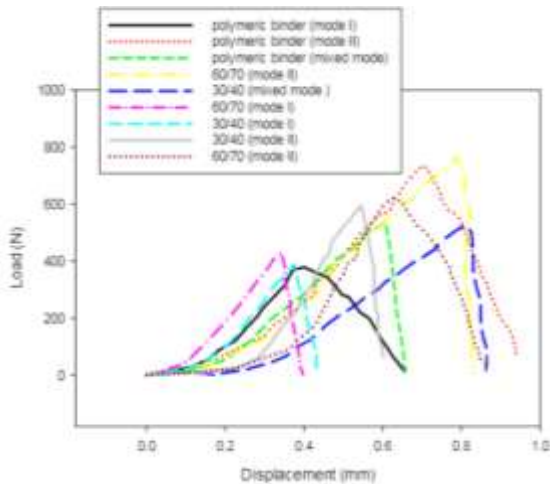


Figure 2.12. Load vs displacement curve of bitumen under mode 1, mode 2 and mixed mode (Aliha 2020)

In order to develop a more environmentally friendly asphalt binder, Sheng et al. (2020) researched the use of flame-retardant composites. Its purpose is to improve the fire resistance of asphalt binder without compromising mixture performance. The following retardant contains four components such as expandable graphite, magnesium hydroxide, calcium hydroxide and ammonium polyphosphate that all react differently to heat. It was determined that the use of the retardants reduced the amounts of heat and carbon monoxide released. Also, it delayed the process of the carbon monoxide from occurring as quickly as it normally did (Figure 2.13) verifying it is in fact environmentally friendly.

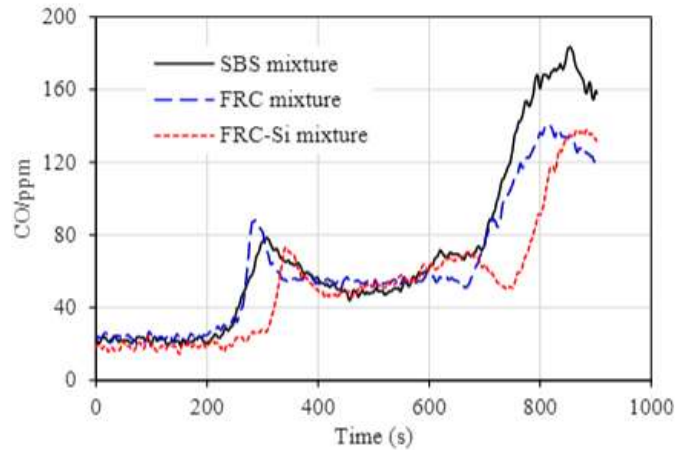


Figure 2.13. Carbon monoxide release curves for SBS, FRC, FRC-Si asphalt (Sheng et al. 2020)

Further testing on a similar topic was conducted by Kasanagh et al. (2020) who investigated a green composite modifier that is produced from the use of recycled materials. They contained high density polyethylene (HDPE), ethylene propylene diene monomers (EPDM), ground tire rubber (GTR) and bitumen. It was stated that composite modifiers could provide both environmental and economic benefits. The binder was tested under various test such as penetration, softening point, viscosity, conventional performance grading, linear amplitude sweep and multiple stress creep recovery. It was concluded that the composite modifiers showed improvements to the rheological properties of the binder.

Raufi et al. (2020) examined binder modification in order to focus on better performing pavements that prevent distresses due to moisture susceptibility and high temperature sensitivity. His research was based on three different nanomaterials: nano-bentonite, nano-CaCo₂ and Zycotherm. It is crucial to state that the addition of nanomaterials causes a change to the optimum binder percentage that was found in this study using the Marshall method. It was determined that the nanomaterials did not cause significant changes to the bitumen. However,

nanomaterials cause the high temperature susceptibility to reduce and allow for greater storage stability of modified binders.

2.6 Fiber-Aggregate-Binder Interlocking

Asphalt pavements experience compression due to the applied loads, which also produce a split tension effect on the opposing axis. As previously mentioned, asphalt mixtures are composed of a skeletal structure produced by the aggregates within the matrix. In FRA materials, the skeletal structure contains fiber additives that are embedded within the mixture. A theory presents that the interlocking of the additives, can contribute to the resistance to the tensile strength and in turn improve the strength parameters of the asphalt.

Park et al. (2015) presented his results in regards to the fiber-aggregate-binder interlocking concept. Figure 2.14 shows the applied forces onto an FRA matrix produced by the applied loads of traffic affliction. The stone-on-stone contact of the skeletal structure is now wedging fibers by means of compression meaning the increase of loads causes an improvement in interlocking. For this reason, longer fibers are more beneficial due to the larger probability of becoming caught between multiple aggregates. Thin fibers are detrimental to the mixture because their diameter is too small to provide enough strength to affect the fiber-aggregate interlocking. This linking system increases the resistance of fiber pull out. It is beneficial to the overall matrix because it has been proved that the asphalt is not strong enough on its own to prevent pull-out. The interlocking mechanism improve the ITS and crack remediation.

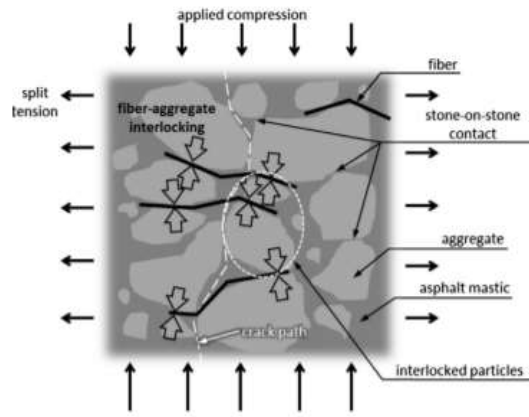


Fig. 13. Schematic view of the reinforcing mechanism.

Figure 2.14. Schematic view of the reinforcing mechanism (Park et al. 2015)

Slebi-Acevedo et al. (2019) explained that the fiber-aggregate interlocking concept is affected by the shape, size and percentage of the fibers. When the correct fiber lengths and binder content is used, stronger connections are created, which lowers the propagation of cracks. The fiber percentage is crucial in determining whether there are enough to create the interlocking mechanism or cause clumping which don't provide the same strength effects. The three-dimensional network strength is improved with the adhesion of the matrix through the following theory. Therefore, providing high flexibility and resistance to fatigue and aging.

When conducting optimization testing, Xu et al. (2010) relates his results to the concept of fiber-aggregate interlocking. He establishes that the polyester and polyacrylonitrile fibers produced the best strength improvement outcomes due to their geometrical and physical properties. The greater length and diameters of the fibers allowed for interweaving to occur to form an efficient networking system. It was also determined that the strength parameters of the FRA increased until a certain point then decreased. He credits this to the excess of fibers that coagulate to form weak points reducing the effects of the interlocking concept.

2.7 Fatigue Testing

Asphalt Concrete is prone to cracking due to factors such as weather conditions, climate, varying mixture designs and placement issues. One of the most common causes of cracking, however, is due to fatigue. As high loads are consistently being applied, cracking initiates on the lower end of the asphalt layer where tensile stress is highest. Cracking will then propagate towards the surface causing cracks to be formed and connected displaying a pattern resembling that of alligator skin. Fatigue cracks deteriorate the integrity and strength of the asphalt mixture; therefore, it is important to test similar loading onto asphalt samples in order to observe how the asphalt will react before placing it onto a large-scale pavement structure. Most fatigue tests are conducted under phenomenological method, mechanical approximation or damage mechanics. It goes hand and hand with the design by which alterations can be changed so that better results are produced for the fatigue tests involved.

Matthews et al. (1993) reviewed various fatigue testing methods and their procedures to define the response of asphalt-concrete mixtures under high loading. The fatigue in asphalt was examined using the following 7 methodologies (Figure 2.15): simple flexure, supported flexure, direct axial, diametral, triaxial, fracture tests and wheel-track tests. It was stated that the simple flexure accounts for the highest percentage of fatigue tests because it is well known, simple and the results can be used directly when designing. It can be conducted through repeated stress and strain at a center point or additional point loads until failure of the specimen occurs. The supported flexure is very similar in loading patterns however it is fully supported at its end which prevents any moments from occurring. Direct axial testing had many factors that played a large role in the results that are obtained. The test must be conducted using short rest periods, consider temperature effects, be tested through sinusoidal load pulse and pure compressive cycling

(Raithby and Sterling 1972). Diametral test are also very common due to their simplicity and the clarity in interpreting the results. This testing method involves applying electrohydraulic or pneumatic loading along the length of the specimen to produce tension along the axis by applying a compressive load. A triaxial test provides the specimen with a confining pressure to simulate stress conditions. Fracture mechanics testing involve tests such as single-edge notched flexure tests and single-edge notched tension tests. Through these tests, the cracking propagation can be closely observed and used to determine the properties of the material. Lastly, wheel-track tests are conducted by applying loads with a pneumatic tire, which is rolled over a specimen to determine the direct effects.

Test	Loading Configuration	Stress Distribution	Loading Waveform	Loading Frequency, cps	Performance Deformation Allowed?	State of Stress	Does failure occur in a Uniform Bending Moment or Tensile Stress Zone?
Third Point Flexure			Reversine Load Rest - 1:9	1-1.67	No	Uniaxial	Yes
Center Point Flexure		Same as above	Sine, Triangular Rectangular Load Rest - 1:100 max	1:100	No	Uniaxial	No
Cantilever			Sine (Bonnot), Sine, Triangular Rectangular Load Rest - 1:100 (van Dijk) max	25 (Bonnot) 1:100 (van Dijk)	No	Uniaxial	No
Rotating Cantilever				16.67	No	Uniaxial	Yes
Test	Loading Configuration	Stress Distribution	Loading Waveform	Loading Frequency, cps	Performance Deformation Allowed?	State of Stress	Does failure occur in a Uniform Bending Moment or Tensile Stress Zone?
Axial				8.33-25.0	No	Uniaxial	Yes
Diametral				1.0	Yes	Biaxial	No
Supported Flexure (Beam)			Reversine	0.75	Yes	Uniaxial	No

Figure 2.15. Summary of fatigue test characteristics (Matthews et al.1993)

Boyer (1986) investigated the fatigue of asphalt concrete mixtures as well the process and effects that are produced. It was determined that fatigue consists of three stages: crack initiation, crack propagation and sudden fracture. Through this research a review was conducted on the various machinery used to test the fatigue processes of asphaltic mixtures. The classification of fatigue testing machines was defined as a direct stress, plane bending, rotating beam, alternating torsion and combined stress. When the direct-stress fatigue test is being utilized a uniform stress and/or strain is produced through the cross section of the specimen. The bending fatigue is tested by applying a load along a small scaled beam to see the reactions of either a single-sided supported or double-sided supported beam. Torsional tests are typically administered by altering linear motion into rotational with the use of machinery. The combined stress test allows for multiple loadings onto a single specimen in different axis as either biaxial or triaxial stresses.

Sramek (2018) conducted two-point bending test to test the fatigue of asphalt using recycled material by finding the deformation characteristics. It was stated that the operational capacity of a roadway is highly dependent on two important factors: deformation and strength characteristic. The former is represented by modulus of elasticity, deformation modulus, modulus of stiffness, creep modulus and poisons ratio while the later can be seen by stability, compressive strength, flexural strength and splitting tensile strength. The complex modulus was used to measure the fatigue because it can appropriately determine the ratio of deformation at steady, harmonically variable oscillations. The Wohler's Diagram, as depicted in Figure 2.16, shows the linear regression of the fatigue life. This diagram was calculated and then used to evaluate the additional parameters of fatigue such as strain, estimated residual standard deviation and correlation coefficient for two asphaltic mixtures. The first asphaltic mixture was categorized as $Fat_{c,min220}$ while the second was $Fat_{c,min115}$. The results showed that the asphaltic

material using recycled material had lower fatigue resistance than that of a mixture using new natural material. However, the complex modulus was higher determining that these mixtures are suitable for maintenance projects. It was stated that the functional fatigue test is critical in designing a proper asphaltic mixture to withstand fatigue and proved to be useful in this study.

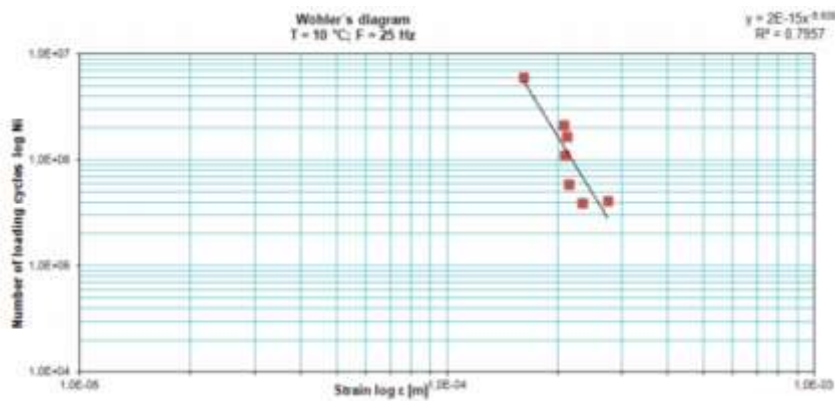


Figure 2.16. Wohler's diagram of the asphalt mixture 1

Fatigue resistance parameters are highly influenced by the asphaltic mixture properties such as aggregate gradation and asphalt properties. Fatigue tests can produce extremely practical results that can interpret how the pavement will react in real life. Li et al. (2019) tested the asphalt properties to determine how they affect the fatigue parameters. The following was carried out for 6 compositions by use of the 4-point bending test, 2-point bending trapezoidal beam and overlay tester. The optimum asphalt content for each method was found using the Marshall mix design. The 2-point bending trapezoidal beam was adapted from European Standards. The overlay tester fatigue was adjusted to follow the Texas standards. The loading method and the model diagram can be seen in Figure 2.17. The results for all three testing methods proved that 6% asphalt mixture was the most appropriate to produce the most suitable pavement to resist fatigue.

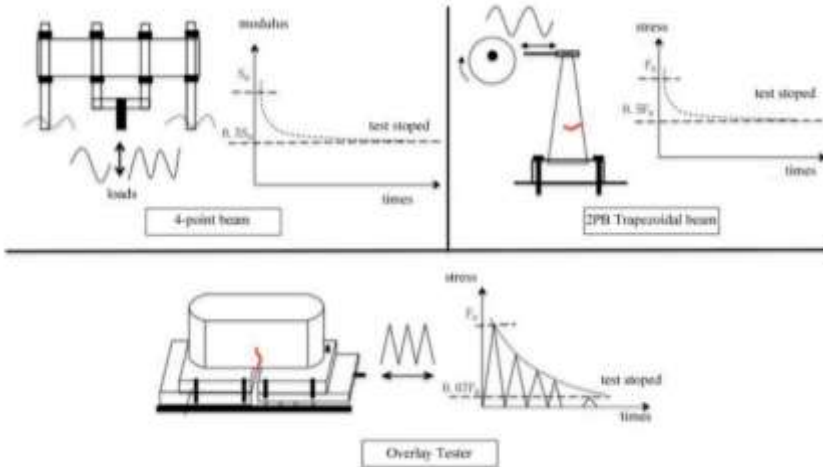


Figure 2.17. Loading method and model diagram (Li et al. 2019)

Meng et al. (2020) conducted fatigue life and life calculations on fiber reinforced concrete maintaining the fiber content and the length-to-diameter ratio as the key components of consideration. The fatigue life of the fiber reinforced samples was conducted under the splitting fatigue test in a controlled stress mode. The stiff modulus parameters were determined in order to define the cumulative damage that was being inflicted on the cylindrical sample. The fatigue damage was classified under three phases: (1) worsened at decreasing rate in the first 12,000 load cycles (2) worsened at constant rate between 12,000 and 64,000 load cycles (3) worsened at an increasing rate after the 64,000 load cycle. During the former stage, the cumulative damage increased at a decreasing rate while the single load cycle damage decreased gradually. The middle stage the cumulative damage increased at a stable rate and the single load cycle damage remained constant. In the latter stage, both the cumulative damage and single load cycle damage increased at a rapid pace. A fatigue life calculation was proposed using the fiber content of the mixture. It combined the formulation of fatigue life of the fiber reinforced asphalt and the k and n values that are dependent on the composition and properties. The fiber content calculation model proved to correlate with the test results and show accuracy.

Fatigue can be tested following various concepts one being dissipated energy. However, many studies have struggled identifying the true dissipation of the sample due to the fact that dissipation could be caused by both fatigue and viscosity of the asphaltic mixture. A concept called the pseudostrain method that studies the dissipated energy by separating the dissipation of viscosity and fatigue in order to identify the true effects that are being acted on the asphalt. The stress-pseudostrain curve is used to calculate the dissipated pseudostrain energy by finding the area under the curve. Varma et al. (2019) conducted additional studies on the dissipated energy concept in order to accurately determine what the fatigue dissipation from a four-point bending test would be. It was suggested that the viscoelastic dissipation remained constant for both damaged and undamaged asphalt conditions. With the alterations made to this process, the inconsistencies seen in previous studies were eliminated. Hence causing a more accurate fatigue dissipation energy calculation.

Fatigue cracking has posed to be one of the most difficult issues in maintaining a high strength asphalt concrete pavement. The iterative cycle of loading and unloading of smaller stresses produce major flaws that impact the overall state of the roadway. Observing the reactions to fatigue is crucial in order to depict the stress and strain reactions of the asphaltic mixture and determine what properties can be improved. Understanding the different testing methods and machine categories is also of great importance in order to ensure that the proper test is being conducted for the results that are being sought out.

2.8 Design

Asphalt is a compound material made of asphaltic binder and aggregates combined to provide a smooth surface that can sustain loading applied by the traveling public. It is the most common

pavement material making up about 94% of U.S. roadways. Although it is more readily available and cost efficient, asphalt pavements deteriorate quicker as opposed to cementitious concrete. For this reason, engineers adapt their asphalt pavement design to accommodate the environment conditions and traffic loading that are associated with that specific pavement. It is important to ensure that the standards for withstanding the outside influences are followed.

Kasianchuk et al. (1970) presented a design subsystem to consider the fatigue mode of distress for asphalt concrete pavements (Figure 2.18). The fatigue subsystem sets up an initial plan and allows others to guide themselves by using the diagram. It ensures that all necessary steps in the design process are taken to ensure that the best pavement design is produced. The design subsystem is divided into three subsections: Preliminary data acquisition, material characterization, analysis and evaluation. The first and one of the most important subsections is Preliminary data acquisition. It involves investigating the properties of the future roadway and its environments. Transportation and environmental factors must be accounted for such as estimated traffic, wheel load distribution, expected growth, subgrade soil survey, weather conditions. The initial design of the asphalt can be then produced using these parameters. The second subsection is Material Characterization. In this portion of the design process, the asphalt concrete, subgrade soil and granular material should be tested for elastic properties. The asphalt concrete should additionally be used to test the fatigue properties. The final subsection, analysis and evaluation, involves examining the variation of stiffness due to weather conditions throughout the year, moisture content of the subgrade, response of the asphalt concrete layer. Its final steps are to predict the fatigue life for fatigue and evaluate the design in regards to fatigue life. Additional mixtures can be produced if changes must be made in order to produce a larger fatigue resistance.

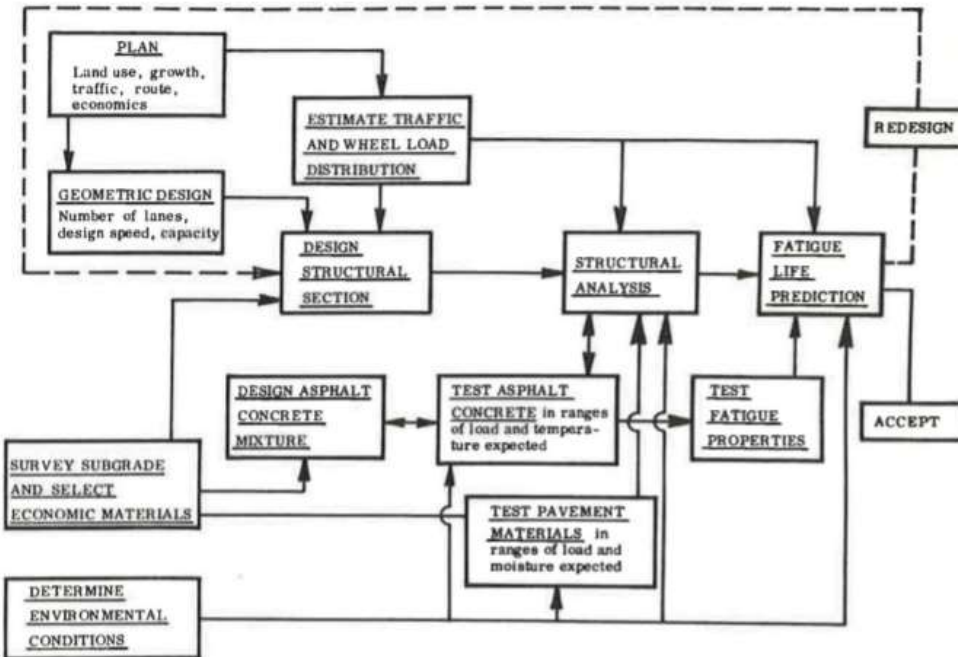


Figure 2.18. Block Diagram of the Design Subsystems (Kasianchuk et al. 1970)

2.9 Degradation of Asphalt

More frequent rehabilitations and reconstruction projects must be carried out for asphalt pavements than that of Portland Cement Concrete. The development of deterioration models provides insight to the dynamics of asphalt and allow for proper scheduling of maintenance works. Therefore, thorough analyzation of deterioration models is crucial and should be conducted in order to determine the performance of asphalt over its lifetime.

Performance prediction models are widely used in infrastructure asset management in order to predict the performance of infrastructure over an allotted time frame. The challenge appears as they have to accurately predict the condition of the actual asphalt pavement conditions. In order to come as close as possible to the most accurate results there are two main types of performance

prediction models used: Deterministic and Probabilistic (Lytton 1987). The former gives an output as a single precise value while the latter gives an output as a range. The deterministic is the most common type of model available and is divided into three subsections. The first is mechanistic which models the actual behavior of pavement and have been used to investigate pavement response. However, it has been criticized for being data intense and for relying on parameters that are too difficult to quantify in real life practices (Prozzi and Madanat 2001). The second is Empirical which uses the dependent variable and relates it to multiple explanatory variables such as traffic load and pavement properties. A weakness attributed is that it is difficult to transfer the model to other locations from its originating location (Patterson 1987). The third is a Mechanistic-Empirical, which combines the best attributes of both mechanistic and empirical to determine the functional forms and explanatory variables. For the probabilistic model, it is commonly seen as Markov Chains, which use the transition matrices to produce a probability output rather than a direct answer (Morosiuk et al. 2004).

Prediction models have been used to demonstrate the deterioration of pavements to allow for proper planning of maintenance as well as implementing regulations to slow down the deterioration process. Deterioration can be seen as cracking surface deformations and disintegration which are based on the asphalt mixture, traffic loads and environmental conditions. The structural modes of deterioration occur within the subgrades and base of the asphalt pavement while nonstructural deteriorations occur on the surface and are seen as rutting and reflective cracks (Merrill et al. 2016). Deterioration modeling can properly predict the deterioration process and allow for more precise preparation to maintain costs low and prevent emergency maintenance costs (Susanna et al. 2017).

Deterioration curves can be very useful because they allow for accurate predictions of future pavement conditions, which then allows for proper planning of maintenance, rehabilitation and reconstruction decisions. If the pavement is not repaired at an appropriate time, there will be substantial increase of the pavement deterioration thus higher costs due to a large amount of emergency maintenance repairs. Accuracy is improved in these models when correct parameters such as climate, precipitation, traffic, loading and pavement are considered in detail. This causes a production of more precise results and can even be used to implement road strategies and policies to reduce deterioration rates.

2.10 Conclusion

The following literature review, contains various studies by qualified researchers that will be used to produce a new study on FRA. Each research report was focused on different testing parameters or specific results that were trying to be produced. Whether their concentration was on the skeletal structure of asphalt, the mechanical properties of FRA or the optimization of fibers, binder or gradation in FRA, the studies contributed to the current knowledge of asphaltic materials. Although each had differing objectives, all the information that was presented will be considered to establish improved testing variables, parameters, environments and materials.

CHAPTER III

MATERIALS AND EXPERIMENTAL METHODS

3.1 Raw Material

The HMA specimens were prepared using limestone aggregate that provides high compressive strength, water absorption and workability (Onchiri 2018). The limestone used was donated for this study by Terra Firma Materials, Valley Caliche Products, and Frontera Material Facility. The following was obtained from Grade 4, 5 and 6 stockpiles from each of the respective asphalt plants (Figure 3.1) with the nominal maximum aggregate size being 1/2" limestone. In addition, fly ash was used as a mineral filler for aggregates passing the Number 200 sieve (0.075 mm).



Figure 3.1. (a) Limestone grade 4, 5 and 6 stockpiles (b) closer view of stockpile

The asphalt binder used for the HMA samples in this study was Performance Grade (PG) 76-22. PG binders are identified by the extreme temperatures that it can withstand. Therefore, the

asphalt binder temperature range is -22°C (-7.6°F) to 76°C (168.8°F). The asphalt used in this study was donated by Valley Caliche Products and Frontera Material Facility.

The fiber additives used in this study as well as their respective properties are shown in Table 3.1. The Dramix OL 13/.20 Fiber was given a Fiber ID of “SF 0.2-13”, which means it is a smooth fiber with 0.2 mm diameter and 13 mm length. Moreover, the Fiber ID “HF 0.55-33” was assigned to the Wirand FS7 Fiber showing it is a hooked fiber with 0.55 mm diameter and 33 mm length.

Table 3.1. Properties of fibers

Fiber ID	Fiber Name	Fiber Type	Cross Sectional Shape	Diameter (mm)	Length (mm)	Aspect Ratio (L/D)	Cross Sectional Area
SF 0.2-13	Dramix OL 13/.20	Smooth	Circular	0.2	13	65	0.031
HF 0.55-33	Wirand FS7	Hooked	Circular	0.55	33	60	0.238

3.2 HMA Design

The Superpave Mix Design Manual (Asphalt Institute 2001) was used to create the HMA gradation mix designs. The ASTM D 3515 standard was used to find the lower and upper limits of the gradation passing percentage for DG mixtures. The D-5 standard was used in order to obtain a 1/2" nominal maximum samples as shown on Table 3.2 (ASTM D3515-01).

Furthermore, the TxDOT standard for SMA mixtures was used as shown in Table 3.3 for 1/2"

nominal maximum aggregate size (TxDOT Item 346). A restricted zone was created using the minimum and maximum limits obtained in the design manual as seen on Table 3.4 (Asphalt Institute 2001).

Table 3.2. Dense mixture D-5 Standard for grading of total aggregate (ASTM D3515-01)

Sieve Number	Sieve Size (mm)	Percent Passing
3/4"	19	100
1/2"	12.7	90-100
No 4	4.75	44-74
No 8	2.36	28-58
No 50	26.52	5-21
No 200	0.075	2-100

Table 3.3. Stone Matrix Asphalt SMA-D medium gradation limits (TxDOT Item 346)

Sieve Number	Sieve Size (mm)	Percent Passing
3/4"	19	100
1/2"	12.7	85-99
3/8"	9.5	50-75
No 4	4.75	20-32
No 8	2.36	16-28
No 16	1.18	8-28
No 30	0.6	8-28
No 50	0.3	8-28
No 200	0.075	8-12

Table 3.4. Minimum and maximum boundaries of sieve size for nominal maximum aggregate size (Asphalt Institute 2001)

Sieve Size Within Restricted Zone	12.5 mm	
	Min	Max
0.300 mm	15.5	15.5
0.600 mm	19.1	23.1
1.180 mm	25.6	31.6
2.360 mm	39.1	39.1

The asphalt binder content using PG 76-22 was determined to be 5.0% for DG and 7.0% for SMA. Chen et al. (2009) determined that the inclusion of fiber additives causes a growth in air void percentage. For proper design, the optimum binder should be altered to account for the additional surface area of the fibers. However, in order to determine the exact effects caused by the fibers, the asphalt binder content is left constant.

Furthermore, the percentage of fiber additives in HMA impact how effective improving the strength parameters will be. If the percentage is low, the fibers will not have the ability to impact the strength. However, if too large of a percentage is incorporated to the mixture, clumping could occur. The lack of uniform distribution would impact the bonding ability in certain areas and cause limited to no improvement in others (Abhati et al. 2010). Park et al (2015) tested fiber reinforced HMA at 0.5%, % 1.0 and % 1.5. Slight clumping occurred at 1.5% fibers by volume and 0.5% fibers did not largely impact the strength parameters. Therefore, it was determined that 1.0% of fiber additives would be used for the following study. The fiber reinforced asphaltic mixture can be seen in Figure 3.2.

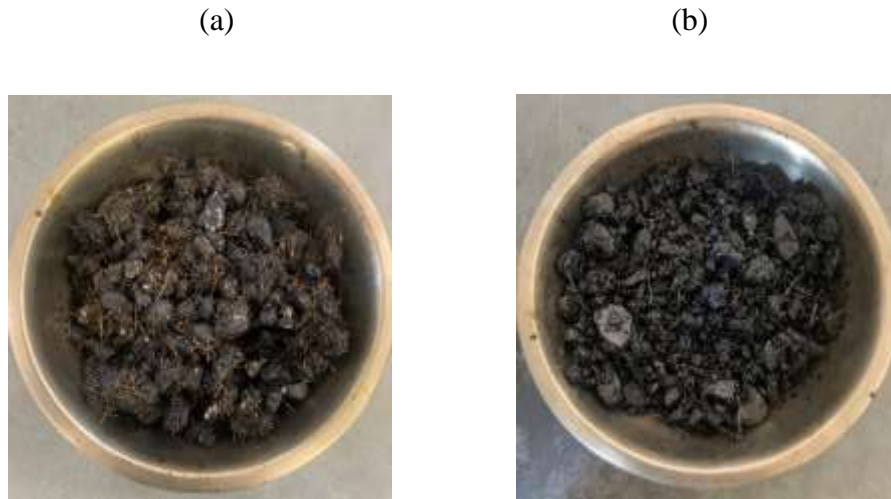


Figure 3.2. (a) SF 0.2-13 in asphaltic mixture (b) HF 0.55-33 in asphaltic mixture

3.3 HMA Specimen Preparation

The limestone aggregate obtained was sieved using the HUMBOLDT Motorized Sieve Shaker following the ASTM standard for sieving fine and coarse aggregates (ASTM C136). The samples were placed on the sieve shaker for approximately 4-6 mins to reach the adequate amount of shaking without causing degradation of the aggregate. The limestone aggregate was separated into smaller stock piles following the respective sizes: 3/4", 1/2", 3/8", No. 4, No.8, No. 16, No. 30, No. 50, No. 200. In order to obtain the weight of each sieve size for the asphalt mixture, an overall aggregate weight of 3000 g was used.

The mixing process of asphalt was conducted by heating the PG 76-22 asphalt to 325 °F as per Tx DOT standards (TEX-205-F). All other items used in the mixing process (aggregate included), were placed into the oven to reach the same mixing temperature. Once completed, the asphalt binder was added into the aggregate mixture until the correct binder percentage was reached. The mixed sample was split into three individual bowls weighing 965 g each. The

following was placed into the oven once again until the molding temperature of 300 °F was reached (TEX-206-F).

The Texas Gyrator Compactor (TGC) was used to mold and compact the cylindrical asphalt samples following the TEX-206-F standards (TEX-206-F). The empty mold was placed in the oven for a minimum of 60 minutes prior to molding. When removed from the oven, it was sprayed with WD-40 to act as a lubricating oil. The asphalt mixture was added between a bottom and top paper lining. Then, the sample was placed onto the TGC and centered directly under the ram. The lever was pulled until 50 psi was reached on the low-pressure gauge. Once obtained, the cam-lever was lowered and the gyrator rotated three times. The process is repeated until 50 psi is attained in one lever pull. Following this, 150 psi is attempted in one concise lever pull. If not obtained, pressure was released to return the low-pressure gauge to 50 psi and gyrated. The process was repeated until 150 psi was obtained in one single pull. When reached, the lever was repeatedly pulled until the high-pressure gauge met 2,500 psi. The pressure was then slowly released and the ram was lifted until the mold was free. The sample was finally removed from the mold obtaining a specimen height of 2 ± 0.06 inches.

The complete specimen preparation process can be observed in Figure 3.3.

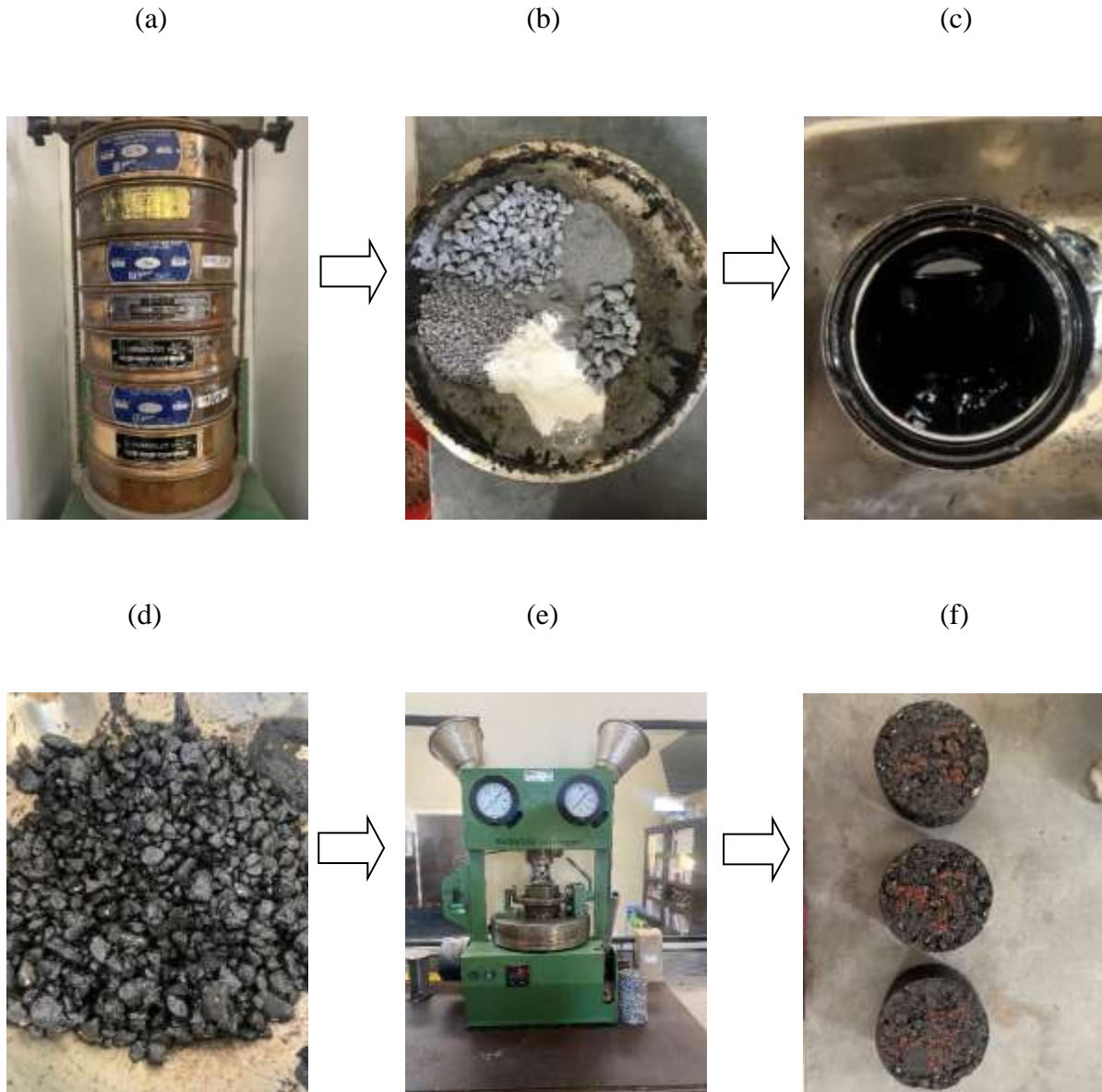


Figure 3.3. Specimen Preparation (a) HUMBOLDT Sieve Shaker (b) Aggregate mixture (c) Heated Asphalt (d) Mixture of Heated Aggregate and Asphalt (e) TGC (f) Sample Molds

3.4 HMA Testing

Indirect tensile tests were conducted to determine the peak load of the HMA samples as the vertical displacement increased uniformly. The Gilson HM-398 Load Frame was used to apply a strain rate of 0.18 in/min. Further, the Karol Warner Data Readout and the Get Data 5.5 software were used to capture, record and display the data. Figure 3.4 demonstrates the setup of the load frame and data reader. When the sample was placed onto the Load Frame, the lower plate was lifted until the load frame and upper plate were 1-3 mm away from each other. The Displacement and Load were tared to bring the values for each to 0. The Get Data test was then started and the Load Frame switch was moved to “Up” to produce constant displacement at the set strain rate. Using the Load and Displacements recorded, the HMA samples were tested to find various strength parameters: cracking resistance, indirect tensile stress, fracture energy, post-cracking energy and toughness. In order to do so, the Indirect Tensile Stress vs Displacement Curves had to be produced using the Load vs Displacement. Equations 1 and 2 were utilized where L is the peak load (lb), t is the sample thickness (in), D is sample diameter (in), Δ is the sample vertical displacement and l is the gauge length (in) (Park et al. 2015). Further, Roque et al. (1997) determined that the fracture energy is the area under the curve up to the strain at the peak load (ϵ_p). The post-cracking energy is represented by the area under the curve after the peak load at the same distance from the peak load ($2\epsilon_p$). While the FE is a good measure of the cracking resistance, the PE is a good indicator of ductility. The toughness can also be determined as the area under the curve from 0 to $2\epsilon_p$ or the sum of FE and PE. The following can be demonstrated in Figure 3.5.

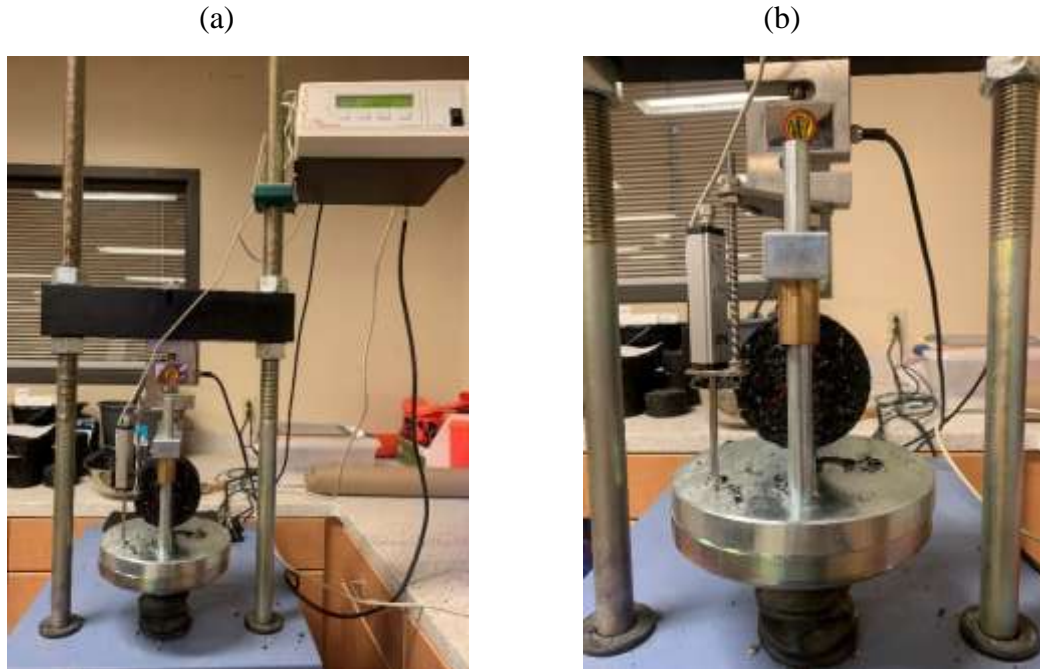


Figure 3.4. (a) Gilson HM-398 Load Frame and Karol Warner Data Readout (b) zoomed view of loading plates

$$\text{Indirect Tensile Stress} = \frac{2*L}{\pi*t*D} \quad (\text{Psi}) \quad [1]$$

$$\text{Strain} = \frac{\Delta}{l} \quad (\text{in/in}) \quad [2]$$

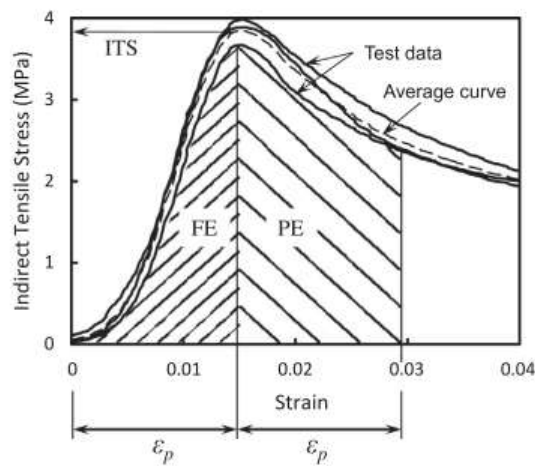


Figure 3.5. ITS, FE and PE description (Park et al. 2015)

CHAPTER IV

INVESTIGATION OF HOT MIX ASPHALT AND THE EFFECTS OF FIBER ADDITIVES

4.1 Production of Fiber Reinforced Hot Mix Asphalt

4.1.1 Gradation Design

Three gradations were produced for both DG and SMA. The three gradations per mixture type were created using a lower, middle and upper limit guide. DG 1 and SMA 1 follow the lower limit meaning it contains a higher percentage of coarse aggregates. In the same manner, DG 3 and SMA 3 follow the upper limit consisting of higher percentages of fine aggregates. The gradation curves for both DG and SMA can be seen in Figure 4.1. The corresponding values for the gradation design of both DG and SMA are also noted in Table 4.1.

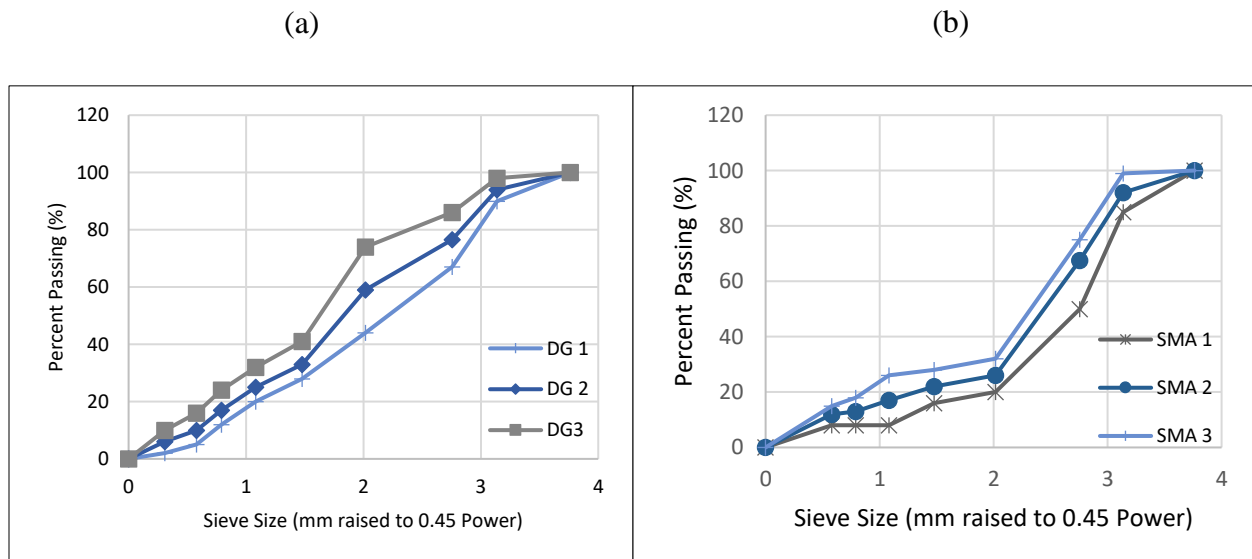


Figure 4.1. Gradation curve for (a) DG asphalt mixtures (b) SMA mixtures

Table 4.1. Gradation Designs for Dense Graded and Stone Matrix Asphalt

Sieve Analysis Sizes			Percent Passing (%)					
	in	mm	DG 1	DG 2	DG 3	SMA 1	SMA 2	SMA 3
Coarse	0.75	19	100	100	100	100	100	100
	0.5	12.7	90	94	98	85	92	99
	0.375	9.51	67	76.5	86	50	67.5	75
	0.187	4.76	44	59	74	20	26	32
Fine	0.0937	2.38	28	33	41	16	22	28
	0.0469	1.19	20	25	32	8	17	26
	0.0234	0.595	12	17	24	8	13	18
	0.0117	0.297	5	10	16	8	12	15
	0.0029	0.074	2	6	10	8	10	12

Based on the gradation charts that were produced as well as their proximity to the restricted area, DG 1 and SMA 1 were chosen to continue the remaining study. DG 1 and SMA 1 contain a smaller percentage of fine aggregates and a larger percentage of coarse aggregate, while remaining in the minimum/maximum limits. This allows for a greater amount aggregate fiber interlocking and a larger percentage of air voids in the mixture that will be beneficial when fiber additives are included. Therefore, moving forward DG 1 will be referred to as DG; similarly, SMA 1 will be SMA.

4.1.3 HMA Properties

HMA properties such as bulk specific gravity, theoretical maximum specific gravity and air void percentage are necessary parameters in determining how each sample reacts under

indirect tensile stress tests. The Bulk Specific Gravity is determined as the ratio of weight of the compacted bituminous mixture specimen to the bulk volume of the specimen and can be found using the TxDOT Determining Density of Compacted Bituminous Mixtures Standards (Tex-207-F). The bulk specific gravity can be calculated using Equation 3 where A, B and C are the weight of the dry specimen (g), weight of the SSD specimen in air (g), and the weight of the specimen in water (g) respectively. The results of the examination are represented in Table 4.2 for DG, DG SF 0.2-13, DG HF 0.55-33 and Table 4.3 for SMA, SMA SF 0.2-13, SMA HF 0.55-33.

$$\text{Bulk Specific Gravity (Ga)} = \frac{A}{B-C} \quad [3]$$

Table 4.2. Bulk specific gravity of DG, DG SF 0.2-13, DG HF 0.55-33

Sample	1	2	3	Average
Dense Graded				
Dry	964.5	964.6	964.8	
Submerged	570.1	570.2	571.0	
SSD	966.4	966.3	966.2	
Bulk SG	2.434	2.435	2.441	2.437
Dense Graded SF 0.2-13				
Dry	964.3	965.0	965.1	
Submerged	549.0	548.2	546.9	
SSD	973.9	974.3	973.5	
Bulk SG	2.269	2.265	2.262	2.266
Dense Graded HF 0.55-33				
Dry	962.4	962.7	963.5	
Submerged	556.0	556.2	560.4	
SSD	976.7	969.5	971.7	
Bulk SG	2.288	2.329	2.343	2.320

Table 4.3. Bulk specific gravity of SMA, SMA SF 0.2-13, SMA HF 0.55-33

Sample	1	2	3	Average
SMA				
Dry	963.6	964.0	962.4	
Submerged	554.4	554.9	554.0	
SSD	966.2	966.5	964.9	
Bulk SG	2.340	2.342	2.342	2.341
SMA SF 0.2-13				
Dry	964.9	964.1	964.4	
Submerged	548.4	548.9	545.2	
SSD	971.1	970.2	970.2	
Bulk SG	2.283	2.288	2.269	2.280
SMA HF 0.55-33				
Dry	964.9	965.8	964.8	
Submerged	554.2	553.7	555.4	
SSD	970.8	971.8	969.8	
Bulk SG	2.316	2.310	2.328	2.318

The theoretical maximum specific gravity for HMA mixtures can be defined as the maximum specific gravity of a bituminous mixture at zero percent air voids. The following parameter can be measured using the Gilson Rice Shaker, Digital Residual Pressure Manometer, and vacuum pump. TxDOT standards for Theoretical Maximum Specific Gravity of Bituminous Mixtures were used to conduct the testing (Tex-227-F). To perform the following test, the

asphaltic mixture must be brought to a workable temperature. The asphalt can then be separated into individual aggregate particles and weighed at dry condition. The metal pycnometer was also filled with water approximately one third full and weighed. The asphaltic mixture is added into the metal pycnometer when room temperature was reached and weighed again to find the weight of the asphalt. The metal pycnometer was then loaded onto the Gilson Rice Shaker and the vibration and vacuum pump were turned on. After 15 minutes, the equipment is turned off and the metal pycnometer is placed in a water bath to find the submerged weight. The theoretical maximum was calculated using Equation 4. A, D and E are represented by the weight of the dry sample in air (g), weight of calibrated pycnometer submerged in water (g) and weight of pycnometer containing the sample while submerged (g). The following values are given in Table 4.4 for DG, DG SF 0.2-13, DG HF 0.55-33 and Table 4.5 for SMA, SMA SF 0.2-13, SMA HF 0.55-33.

$$\text{Theoretical Maximum Specific Gravity (Gmm)} = \frac{A}{D+A-E} \quad [4]$$

Table 4.4. Theoretical maximum specific gravity of DG, DG SF 0.2-13, DG HF 0.55-33

DG	
Weight of Dry Sample in Air	1049.6
Weight of Calibrated Pyc w/ H2O	1377.9
Weight of Sample, Pyc and H2O	2009.8
Rice Specific Gravity	2.513
DG SF 0.2-13	
Weight of Dry Sample in Air	1043.3
Weight of Calibrated Pyc w/ H2O	1377.9
Weight of Sample, Pyc and H2O	2010.5
Rice Specific Gravity	2.540
DG HF 0.55-33	
Weight of Dry Sample in Air	1050.1
Weight of Calibrated Pyc w/ H2O	1377.9
Weight of Sample, Pyc and H2O	2012.6
Rice Specific Gravity	2.528

Table 4.5. Theoretical maximum specific gravity of SMA, SMA SF 0.2-13, SMA HF 0.55-33

SMA	
Weight of Dry Sample in Air	1048.4
Weight of Calibrated Pyc w/ H2O	1377.9
Weight of Sample, Pyc and H2O	1992.8
Rice Specific Gravity	2.418
SMA SF 0.2-13	
Weight of Dry Sample in Air	1049.8
Weight of Calibrated Pyc w/ H2O	1377.9
Weight of Sample, Pyc and H2O	2020.1
Rice Specific Gravity	2.576
SMA HF 0.55-33	
Weight of Dry Sample in Air	1050.3
Weight of Calibrated Pyc w/ H2O	1377.9
Weight of Sample, Pyc and H2O	2019.6
Rice Specific Gravity	2.570

The air void percentage of asphalt is a critical aspect as low air void content would lead to inadequate room for expansion of the asphalt binder under high temperatures. The low air void content would also cause plasticity and in turn lose its strength. Further, high air void contents would remove the ability for aggregates to interlock losing strength as well. The air void percentages calculations are seen in Table 4.6 for DG, DG SF 0.2-13, DG HF 0.55-33 and Table 4.7 for SMA, SMA SF 0.2-13, SMA HF 0.55-33. The values were determined using Equation 5.

$$\text{Air Void } (Va) = \frac{G_{mm} - G_{mb}}{G_{mm}} \quad [5]$$

Table 4.6. Air void percent of DG, DG SF 0.2-13, DG HF 0.55-33

DG	
Bulk Specific Gravity	2.437
Theoretical Maximum Specific Gravity	2.513
Air Void (%)	3.017
DG SF 0.2-13	
Bulk Specific Gravity	2.265
Theoretical Maximum Specific Gravity	2.540
Air Void (%)	10.837
DG HF 0.55-33	
Bulk Specific Gravity	2.32
Theoretical Maximum Specific Gravity	2.528
Air Void (%)	8.225

Table 4.7. Air void percent of SMA, SMA SF 0.2-13, SMA HF 0.55-33

SMA	
Bulk Specific Gravity	2.341
Theoretical Maximum Specific Gravity	2.418
Air Void (%)	3.203
SMA SF 0.2-13	
Bulk Specific Gravity	2.28
Theoretical Maximum Specific Gravity	2.576
Air Void (%)	11.476
SMA HF 0.55-33	
Bulk Specific Gravity	2.318
Theoretical Maximum Specific Gravity	2.570
Air Void (%)	9.822

The HMA molded samples were tested using the Gilson HM-398 Load Frame with the strain rate being set at 0.18 in/min and the sample time set at 1 second. The following settings allowed for over 200 intermediate reading producing a smooth and consistent Load vs Displacement curve. Figure 4.2 and Figure 4.3 display the Indirect Tensile Stress vs Strain for DG, DG SF 0.2-13, DG HF 0.55-33 and SMA, SMA SF 0.2-13, SMA HF 0.55-33 respectively. Three samples are produced for each mixture type to prove consistency. However, as shown, an average value was obtained that will be presented during future results.

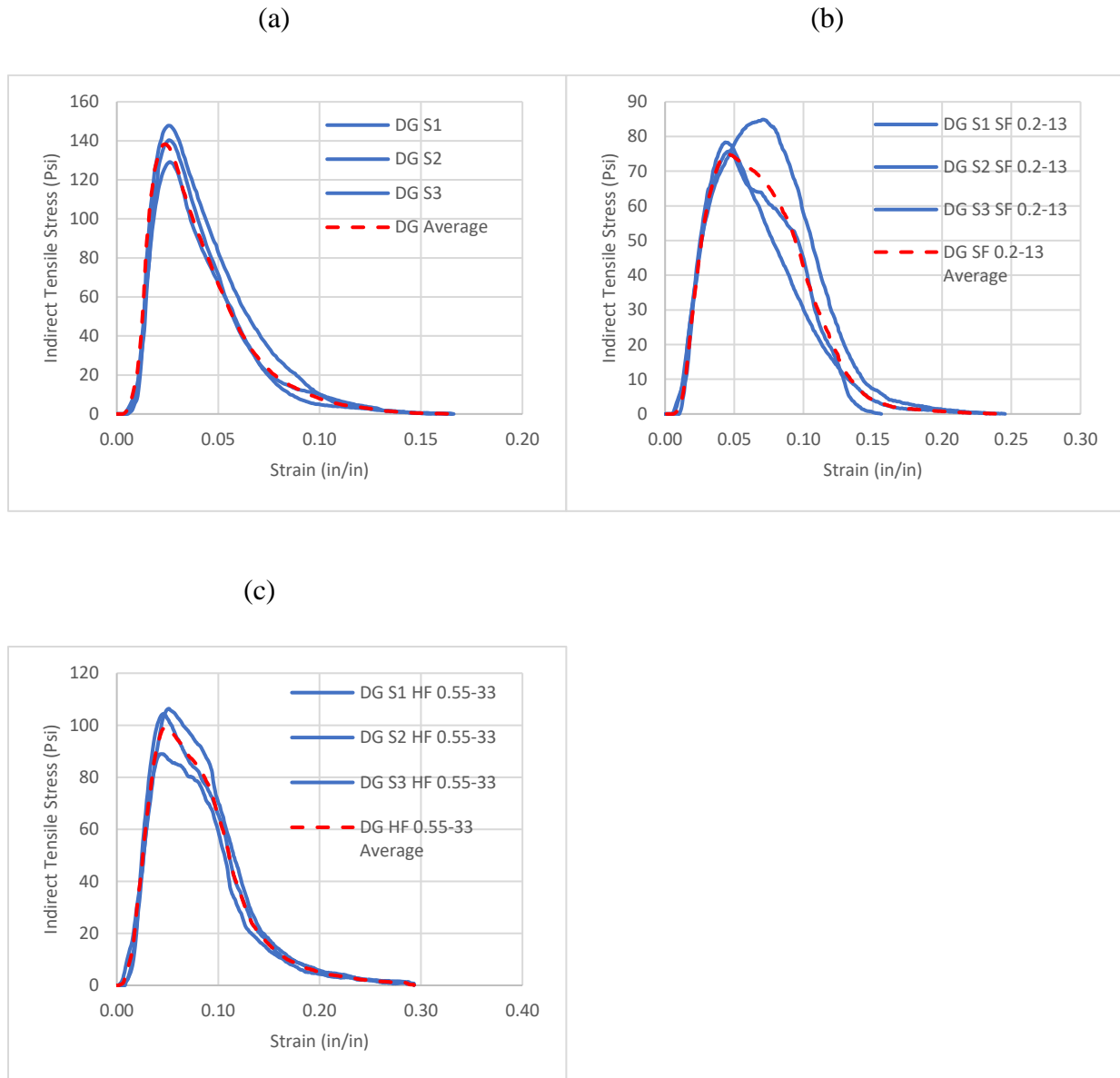


Figure 4.2. ITS vs strain curve for (a) DG (b) DG SF 0.2-13 (c) DG HF 0.55-33

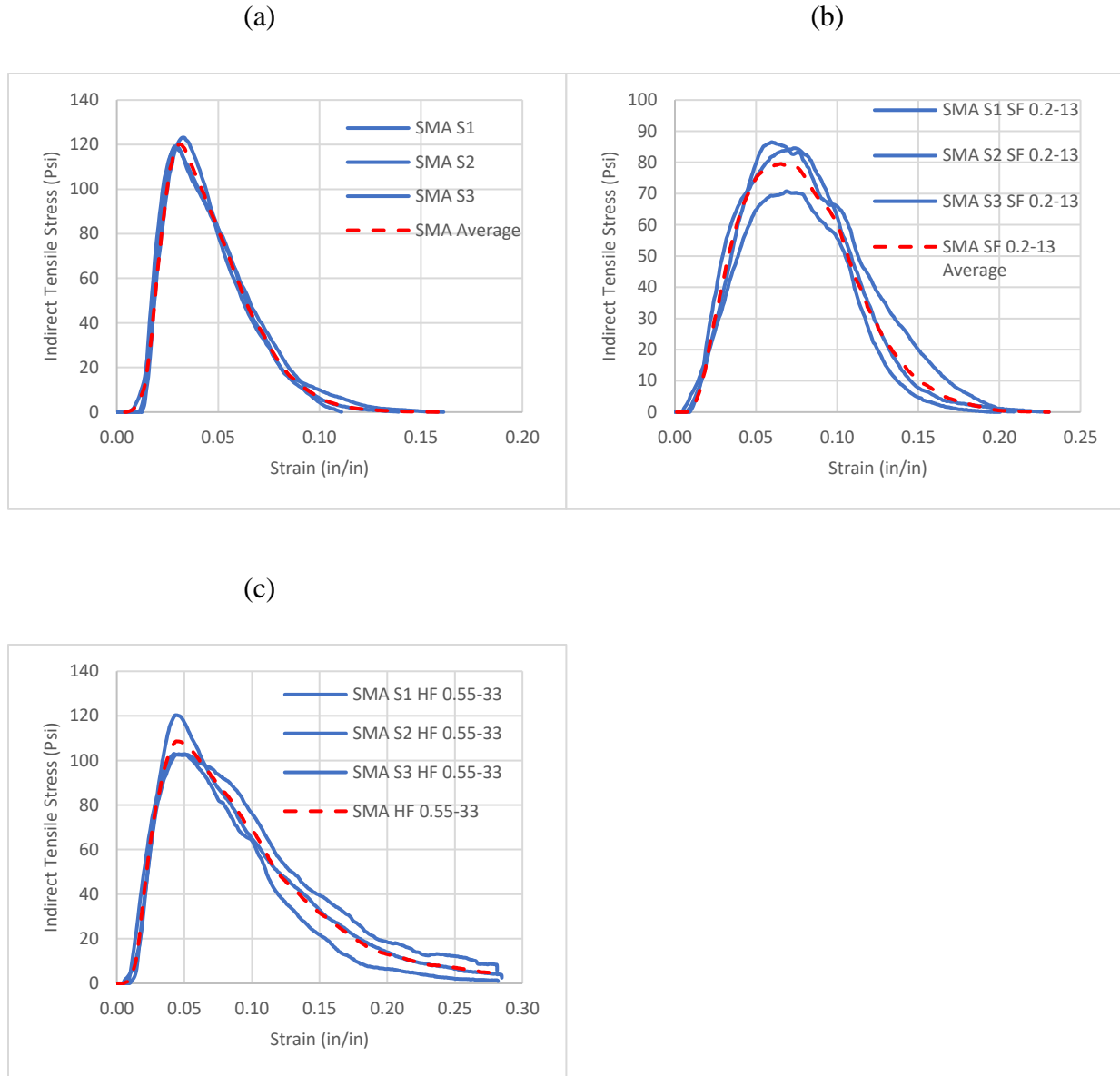


Figure 4.3. ITS vs strain curve for (a)SMA (b) SMA SF 0.2-13 (c) SMA HF 0.55-33

4.2 Investigation of Fiber Additives

Through the indirect tensile test, it was evident that the fiber additives increased the testing time of the HMA specimens meaning the durability increased. The cracking experienced was direct cracking from the center to center of the specimens as seen on Figure 4.4. However,

the bottom of the specimens remained intact after the test was conducted demonstrating that the fiber additives provide extra reinforcement in maintaining compaction. It could also be noted that the fiber reinforced HMA specimens experienced a substantial amount of pulverized aggregate which show that during loading, the aggregate is being broken down around the fibers. The following is consistent with ITS cracking results seen by Park et al. (2015).

(a)



(a)



(c)



Figure 4.4. (a) Broken Fiber Reinforced HMA specimens after ITS test (b) Fractured surface of SF 0.2-13 (c) Fractured surface of HF 0.55-33

The effects of the addition of fiber additives are seen through the indirect tensile stress vs strain curves of non-reinforced DG and SMA compared to steel fiber reinforced samples. It is apparent that the fiber additives caused the ITS to decrease (Figure 4.5). However, this can be attributed to the increase of air voids due to the constant 5.0% and 7.0% asphalt binder for DG and SMA respectively. The decrease of ITS could also have been affected by the compaction method of the Texas Gyrator Compactor that produces molds based on pressure rather than gyrations and air void content. The graphs make it evident that the hooked fiber with a larger diameter and length improved the strength of the HMA for both DG and SMA. Although the DG mixture had a 16% higher ITS than SMA, the SMA SF 0.2-13 had an about 6% higher ITS than DG SF 0.2-13. Similarly, SMA HF 0.55-33 had an about 9% higher ITS value than SMA SF 0.55-33. The following proves that the HF 0.55-33 had the largest effects to the overall ITS.

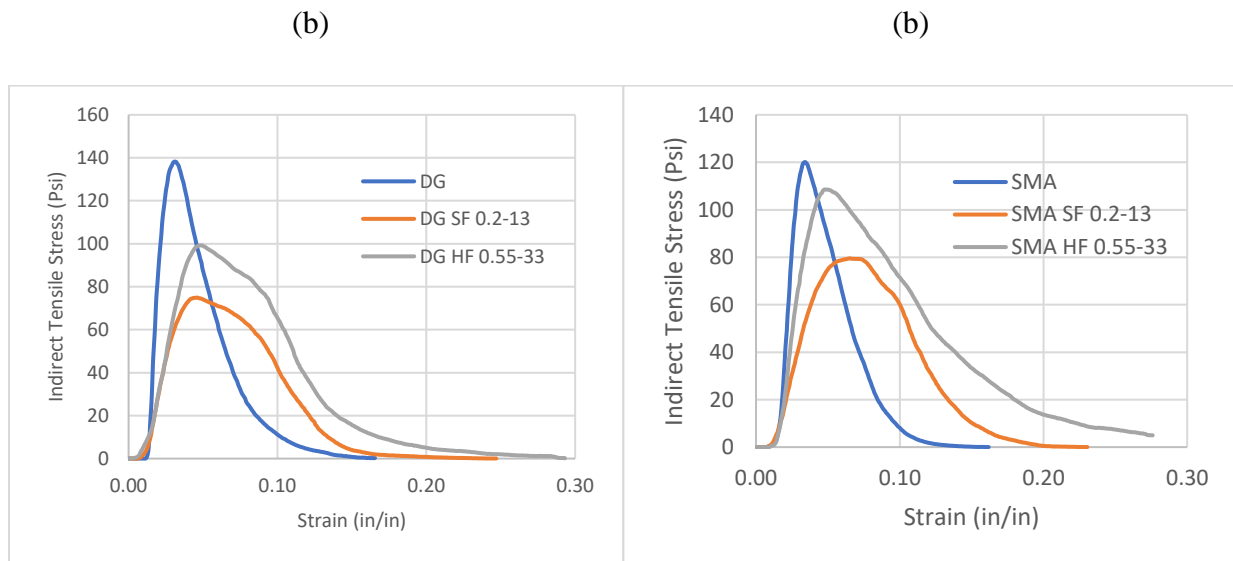


Figure 4.5. ITS vs strain curve for averaged (a) DG, DG SF 0.2-13, DG 0.55-33 (b) SMA, SMA SF 0.2-13, SMA 0.55-33

The Indirect Tensile Stress vs Strain curves give insight to the cracking resistance of asphalt samples. Regardless of the decrease in ITS, the addition of fibers caused an increase of

fracture energy and post-cracking energy of HMA (Figure 4.6). As a result, the HMA specimens showed an increase in toughness (sum of FE and PE). DG SF 0.2-13 had a 14% increase in toughness while DG HF 0.55-33 produced a 70% increase. On the other hand, SMA SF 0.2-13 had a 67% increase compared to the non-reinforced mixture while SMA 0.55-33 had a 58% increase. It is noted that a larger increase is experienced for the post-cracking energy meaning that after initial cracking, fiber additives are enduring the applied load.

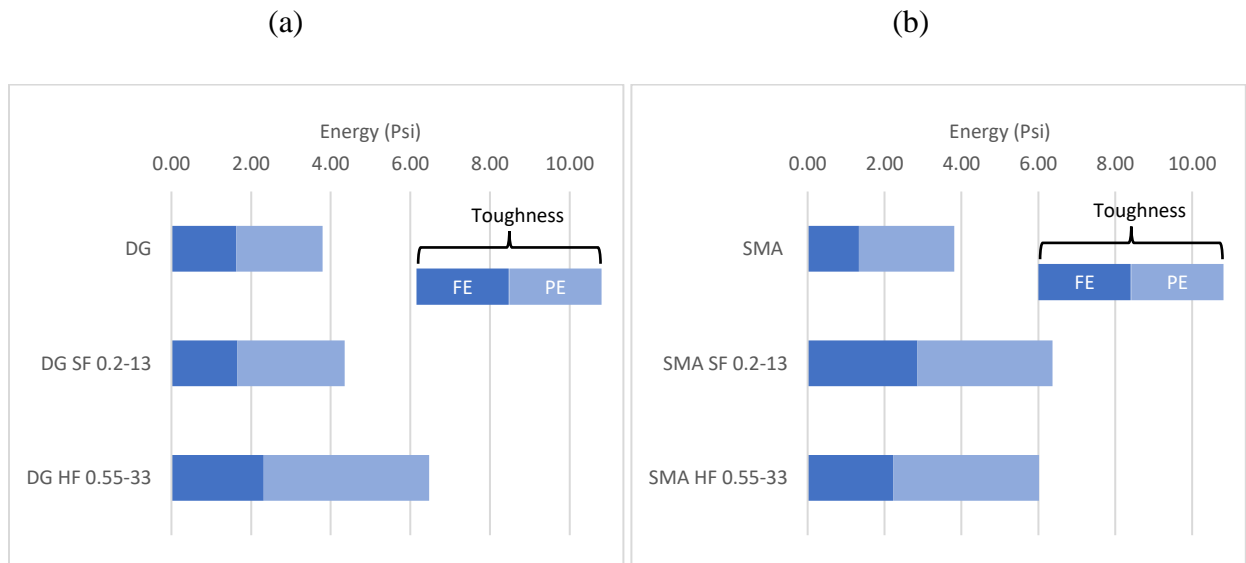


Figure 4.6. FE, PE and toughness for averaged (a) DG, DG SF 0.2-13, DG 0.55-33 (b) SMA, SMA SF 0.2-13, SMA 0.55-33

4.3 Discussions on the effects of fiber additives on HMA

The indirect tensile tests of fiber reinforced HMA proved that the addition of fibers positively impact cracking resistance. A summary of results can be seen in Table 4.8 showing ITS, FE, PE, toughness and air voids. The fiber reinforced HMA showed a decrease in the ITS; however, previous studies have shown otherwise. The decrease in ITS is assumed to be attributed to the lack of accountability for additional surface area for optimum asphalt content and

insufficient compaction for reinforced specimens. The ITS results showed that the HF 0.2-13 increased the ITS value more than the SF 0.2-13 in both the DG and SMA. Further, the increase in fracture energy and post-cracking energy proved that cracking resistance is impacted by the fiber additives. The increase in post-cracking stress in particular proved that fiber reinforced HMA are more ductile. The ductility improvements will cause improvements in the HMA lifetime by decreasing fatigue and in turn reducing rutting experienced. The results showed that the DG mixture had a largest increase in toughness when HF 0.55-33 was included. On the other hand, the SMA mixture experienced a larger increase in toughness with the use of SF 0.2-13. The mixture type also proved to be a crucial factor on the effects of fiber additives as SMA saw greater results. It could be assumed that the large percentage of coarse aggregates in SMA mixtures allow for more fiber-aggregate-interlocking.

Table 4.8. Summary of ITS, FE, PE and toughness for DG and SMA

Asphalt Type	DG			SMA		
Fiber ID	Non-Reinforced	SF 0.2-13	HF 0.55-33	Non-Reinforced	SF 0.2-13	HF 0.55-33
Volume Content of Fiber, Vf (%)	1.0	1.0	1.0	1.0	1.0	1.0
Indirect Tensile Strength, ITS (Psi)	138.24	74.92	99.23	120.12	79.54	108.57
Fracture Energy, FE (Psi)	1.63	1.65	2.32	1.33	2.86	2.22
Post-Cracking Energy, PE (Psi)	2.17	2.70	4.15	2.48	3.51	3.79
Toughness (Psi)	3.80	4.35	6.47	3.81	6.37	6.02
% Air Voids	3.02	10.82	8.23	3.20	11.47	9.82

CHAPTER V

CONCLUSION AND FUTURE WORK

5.1 Conclusion

In this study, the effects of adding fibers in hot-mix asphalt was investigated. Both dense graded asphalt mixtures and Stone Matrix Asphalt mixtures containing steel fibers of different shapes and size were examined and compared to the non-reinforced control specimen. The 4-inch diameter cylindrical samples were tested through indirect tension tests to determine cracking resistance including indirect tension strength, fracture energy, post-cracking energy and toughness. The results of all samples were then used to determine the effectiveness of fiber reinforcement.

The test results showed that the addition of fibers improves the fracture energy and post-cracking energy but decreases the indirect tensile strength. The improvements in fracture energy and post-cracking energy were observed by both fiber types and mixtures. In dense-graded mixtures, longer fibers (HF 0.55-33) caused a larger improvement than the shorter fibers (SF 0.2-13). On the other hand, in SMA, both fibers showed similar improvements in toughness (fracture energy + post-cracking energy) while shorter fibers (SF 0.2-13) showed slightly higher improvements than longer fibers. The increases in toughness verify that the cracking resistance is impacted by the addition of fibers as the HMA becomes more ductile. On the other hand, that the decreases in indirect tensile strength were presumed to be caused by insufficient compaction and

changes in optimum binder content of the fiber reinforced specimens. The percent air voids of fiber reinforced specimens were much higher than the control specimens, and this implies that 1) optimum binder content should be adjusted and 2) higher compaction efforts are needed when adding fibers into HMA.

The results presented in this study show that 1) adding fibers has potentials to improve cracking resistance of HMA and 2) special cares in compaction and determination of optimum binder content will be needed to achieve proper air-void contents. Although the research gives insights to the effects of fiber reinforcement and the impacts of the skeletal structure, further investigation is suggested to ensure adequacy and consistency.

5.2 Recommendations for Future Work

Based on the study conducted, it was determined that future work could be conducted to verify the results. Studies on the optimization of asphalt content to account for the additional fiber additives' surface area could lower the air void content to the acceptable 3.0%- 8.0% range and possibly reach the exact air void content of the non-reinforced specimens. To ensure that the SMA mixture had a larger effect on the indirect tensile strength, fracture energy, post-cracking energy and toughness than the DG mixture due to fiber aggregate interlocking. 2D and 3D modeling of aggregate contact points and fiber aggregate interlocking would be beneficial. Conducting similar tests with various SMA and DG samples would also provide consistency to verify the produced results.

REFERENCES

- Abtahi, S. M., Sheikhzadeh, M., Hejazi, S. M., 2010. Fiber-reinforced asphalt-concrete – A review. *Construction and Building Materials*, 24, 871-877.
- Anurag, K., Xiao, F., Amirkhanian, S. N., 2009. Laboratory investigation of indirect tensile strength using roofing polyester waste fibers in hot mix asphalt. *Construction and Building Materials*, 23, 2035-2040.
- Asphalt Institute, 2001. Superpave Mix Design. *Asphalt Institute Superpave Series No. 2, Third Edition*.
- ASTM C136 / C136M -14, Standard Test Method for Sieve Analysis of Fine and Coarse Aggregates, ASTM International, West Conshohocken, PA, 2017.
- ASTM D3515-01, Standard Specification for Hot-Mixed, Hot-Laid Bituminous Paving Mixtures, ASTM International, West Conshohocken, PA, 2001.
- Boyer, H. E., 1986. Fatigue testing. Report of ASM International, USA. 1-10.
- Button, J. W. And Lytton, R. L., 1987. Evaluation of fabrics, fibers and grids in overlays. Proceedings, sixth International Conference Structural Design of Asphalt Pavements, 1, 925-934.
- Cai, X., Wu, K. H., Huang, W. K., Wan, C., 2018. Study on the correlation between aggregate skeleton characteristics and rutting performance of asphalt mixture. *Construction and Building Materials*, 179, 294-301.
- CAPA. Volumetrics in Asphaltic mixtures, Colorado Asphalt Pavement Association.
- Chen H., Xu, Q., Chen S. And Zhang, Z., 2009. Evaluation and design of fiber-reinforced asphalt mixtures. *Materials and Design*, 30, 2595-2603.
- Grasely, Z.C. And Yazdanbakhsh, A., 2011. Quantifying the dispersion of discrete inclusions in composites using continuum theory. *Composites: Part A*, 42, 2043-2050.
- Jaskula, P., Stienss, M., Szydłowski, C., 2017. Effect of polymer fibres reinforcement on selected properties of asphalt mixtures. *Procedia Engineering*, 172, 441-448.

- Kasanagh, S. H., Ahmedzade, P., Fainleib, A. M., Behnood, A., 2020. Rheological properties of asphalt binders modified with recycled materials: A comparison with Styrene-Butadiene-Styrene (SBS). *Construction and Building Materials*, 230, 117047.
- Kasianchuk, D. A., Monismith, C.L., Garrison, W.A., 1970. Asphalt Concrete Pavement Design- A subsystem to consider fatigue mode of stress. Committee on Theory of Pavement Design. 48th Annual Meeting.
- Kennedy, C.J., Revie, W. A., Troalen, L., Wade, M., Wess, T. J., 2013. Studies of hair for use in lime plaster: Implications for conservation and new work. *Polymer Degradation and Stability*, 98, 894-898.
- Kim, K.W., Doh, Y. S., Lim, S., 1999. Mode I reflection cracking resistance of strengthened asphalt concretes. *Construction and Building Materials*, 13, 243-251.
- Li, K., Huang, M., Zhong, H., Li, B., 2019. Comprehensive evaluation of Fatigue Performance of Modified Asphalt Mixtures in Different Fatigue Tests. *Applied Science*, 9, 1850.
- Li, P., Su, J., Ma, S., Dong, H., 2020. Effect of aggregate contact condition on skeleton stability in asphalt mixture. *International Journal of Pavement Engineering*, 21(2), 196-202.
- LI, Y. X., 2013. Study on the slippage and shearing behavior of Asphalt mixture aggregate. Thesis (MA). Chang'an University.
- Liu, Y., Su, P., Li, M., You, Z., Zhao, M., 2020. Review on evolution and evaluation of pavement structures and materials. *Journal of Traffic Transportation Engineering*, 7(5), 573-599.
- Lytton, R. L., 1987. Concepts of Pavement Performance Prediction and Modeling. Proceedings Second North American Conference on Managing Pavement, 2.
- Ma, T., Zhen, W. And Yong-Li, Z., 2011. Degradation behavior of aggregate skeleton in stone matrix asphalt mixture. *Central South University of Technology*, 18, 2192-2200.
- Mahrez, A., Karim, M. R., Katman, H. Y., 2005. Fatigue and deformation properties of glass fiber reinforced bituminous mixes. *Journal of the Eastern Asia Society for Transportation Studies*, 6, 997-1007.
- Matthews, J. M., Monismith, C.L., Craus, J., 1993. Investigation of Laboratory Fatigue Testing Procedures for Asphalt Aggregate Mixtures. *Journal of Transportation Engineering*, 119 (4), 634-654.

- Meng, F., Gao, D., Chen, F., Huang, C., 2020. Fatigue Performance Test and Life Calculation of Fiber-Reinforced Asphalt Concrete. *International Information and Engineering Technology Association*, 44 (2), 133-139.
- Morosiuk, G., Riley, M. Odoki, J.B., 2004. Modelling road deterioration and works effects. Highway Development and Management. HDM-4 Series of Publications. Vol. 6.
- National Asphalt Pavement Association, 2013. Fast Facts. *National Asphalt Pavement Association*, 1-2.
- O'flaherty, C. And Hughes D., 2015. Highways: The location, design, construction and maintenance of road pavements, Fifth edition. Ice Publishing. 567p.
- Onchiri, R.O., 2018. Structural Performance of limestone as an aggregate for lightweight concrete. *International Journal of Engineering Research & Technology*, 7(11), 218-221.
- Park, P., El-Tawil, S., Naaman, A. E., 2017. Pull-out behavior of straight steel fibers from asphalt binder. *Construction and Building Materials*, 144, 125-137.
- Park, P., El-Tawil, S., Park, S. Y., Naaman, A. E., (2015). Cracking resistance of fiber reinforced asphalt concrete at -20°C. *Construction and Building Materials*, 81, 47-57.
- Pasetto, M. And Baldo, N., 2014. Influence of the aggregate skeleton design method on the permanent deformation resistance of stone mastic asphalt. *Materials Research Innovations*, 18(3), S3-96-S3-101.
- Paterson, W. D. O., 1987. Road deterioration and maintenance effects models for planning and management. *Washington, DC: The International Bank for Reconstruction and Development*, 1-466.
- Pouranian, M. R. And Haddock, J. E., 2018. Determination of voids in the mineral aggregate and aggregate skeleton characteristics of asphalt mixtures using a linear-mixture packing model. *Construction and Building Materials*, 188, 292-304.
- Prozzi, J.A. And Madanat, S., 2001. Nonlinear model for predicting pavement performance before and after rehabilitation. Proceedings of the second international symposium on maintenance and rehabilitation of pavements and technological control. 1-17.
- Pszczola M. And Szydlowski, C., 2018. Influence of Bitumen Type and Asphalt Mixture Composition on Low-Temperature Strength Properties According to Various Test Methods. *Materials*, 11, 2118.

- Raithby, K. D. And Sterling, A. B., 1972. Some effects of loading history on the performance of rolled asphalt. TRRL-LR 496.
- Raufi, H., Topal, A., Sengoz, B. And Kaya, D., 2020. Assesment of Asphalt Binders and Hot Mix Asphalt Modified with Nanomaterials. *Periodica Polytechnica Civil Engineering*, 64(1), 1-13.
- Roque, R., Buttlar, W.G., Ruth, B.E., Tia, M., Dickinson, S.W., Reid, B., 1997. Evaluation of SHRP indirect tension tester to mitigate cracking in asphalt pavements and overlays – final report to the Florida department of transportation. Gainesville, FL: University of Florida.
- Serin, S., Morova, N., Saltan, M., Terzi, S., 2012. Investigation of usability of steel fibers in asphalt mixtures. *Construction and Building Materials*, 36, 238-244.
- Sheng, Y., Wu, Y., Yan, Y., Jia, H., Qiao, Y., Underwood, B. S., Niu, D., Kim, Y. R., 2020. Development of environmentally friendly flame retardant to achieve low flammability for asphalt binder used in tunnel pavements. *Journal of Cleaner Production*, 257, 120487.
- Shukla, M., Tiwari, D., Sitaramanjaneyulu K., 2014. Performance characteristics of fiber modified asphalt concrete mixes. *The International Journal of Pavement Engineering and Asphalt Technology*, 15(1), 38-50.
- Slebi-Acevedo, C. J., Lastra-Gonzalez, P., Pascual-Munoz, P., Castro-Fresno, D., 2019. Mechanical Performance of fibers in hot mix asphalt: A review. *Construction and Building Materials*, 200, 756-769.
- Sramek, J., 2018. Stiffness and Fatigue of Asphalt Mixtures for Pavement Construction *Slovak Journal of Civil Engineering*. 26(2), 24-29.
- Tapkin, S., 2008. The effect of polypropylene fibers on asphalt performance. *Building and Environment*, 43, 1065-1071.
- TxDOT Designation: Item 346, Standard Specification for Stone Matrix Asphalt, Texas Department of Transportation.
- TxDOT Designation: TEX-205-F, Laboratory Method of Mixing Bituminous Mixtures, Texas Department of Transportation.
- TxDOT Designation: TEX-206-F, Compacting Specimens using the Texas Gyrator Compactor, Texas Department of Transportation.

TxDOT Designation: TEX-207-F, Determining Density of Compacted Bituminous Mixtures, Texas Department of Transportation.

TxDOT Designation: TEX-227-F, Theoretical Maximum Specific Gravity of Bituminous Mixtures, Texas Department of Transportation.

Vargas, J., Bariola, J., Blondet, M., 1986. Seismic Strength of Adobe Masonry. *Materials and Structures*, 9(4), 253–256.

Varma, R., Naratan, S. P. A., Krishnan, J. M., 2019. Quantification of Viscous and Fatigue dissipation of asphalt concrete in four-point bending tests. *Journal of Materials in Civil Engineering*, 31(12), 1 – 12.

Westman, A. E. R., 1936. The packing of particles: empirical equations for intermediate diameter ratios. *Journal of American Ceramic Society*, 19, 127-129.

Wu, S., Ye, Q., Li, N., Investigation of rheological and fatigue properties of asphalt mixtures containing polyester fibers. *Construction and Building Materials*, 22(10), 2111-5.

Xu, Q., Chen, H., Prozzi, J. A., 2010. Performance of fiber reinforced asphalt concrete under environmental temperature and water effects. *Construction and Building Materials*, 24, 2003-2010.

Zhang, H., Anupam, K., Scarpas, A., Kasbergen, C., Erkens, S., 2019. Effect of Stone on Stone Contact on porous asphalt mixes: micromechanical analysis. *International Journal of Pavement Engineering*, 2019.

Zube, E., 1956. Wire mesh reinforcement in bituminous resurfacing. *High Res Rec Bull*, 131, 1-18.

BIOGRAPHICAL SKETCH

Samantha Avila was born and raised in Laredo, Texas on 18th August 1998. She graduated in December of 2019 with a B.S. in Civil Engineering from the University of Texas Rio Grande Valley where she was a UTRGV Scholar and obtained Summa Cum Laude honors. Avila then continued her education and earned a M.S. in Civil Engineering with a focus on Construction and Structures in December of 2021. This was also completed at The University of Texas Rio Grande Valley where she was a Presidential Graduate Research Assistant Scholar. During her graduate program, she worked as a research assistant for two years and as a teacher assistant during her second year. Her thesis investigated the skeletal structure of asphalt as well as the interactions with fiber additives.

Avila has gained professional experience through four summer internship programs with the Texas Department of Transportation and one with Jacobs Engineering Group. While working under licensed engineers, she was exposed to various aspects of engineering such as design, transportation, construction, survey and project management.

Email: SamanthaAAvila12@gmail.com; Samantha.Avila01@utrgv.edu